A Real-time Vehicle-Specific Eco-Routing Model for On-board Navigation Applications Capturing Transient Vehicle Behavior

Jinghui Wang[a], Ahmed Elbery[b], Hesham A. Rakha[c,*]

[a]*National Renewable Energy Laboratory, 15013 Denver West Parkway, Golden, CO 80227, USA*
[b]*Center for Sustainable Mobility, Virginia Tech Transportation Institute, 3500 Transportation Research Drive, Blacksburg, VA 24061, USA*
[c]*Center for Sustainable Mobility, Virginia Tech Transportation Institute, 3500 Transportation Research Drive, Blacksburg, VA 24061, USA*

Abstract

The paper develops a real-time vehicle-specific eco-routing model for use in on-board navigation systems for both conventional fuel- and battery-powered electric vehicles. The model uses a novel link cost function that retains all microscopic transient behavior along a link by capturing within-link speed, acceleration, and road grade variations. Specifically, eight vehicle-agnostic link-specific variables are transmitted to the cloud and fused with information received from other connected vehicles. The fused data are then sent back to the connected vehicles and used to compute vehicle-specific eco-routes (edge computing). The solution produces an energy-efficient dynamic user-equilibrium traffic assignment that is solved incrementally. A numerical experiment is first designed to test the model, demonstrating the benefits associated with vehicle-specific eco-routes compared to those produced by traditional models. The model is then implemented in a micro-simulation framework to evaluate the network-wide impacts of the proposed energy-efficient user-optimum incremental traffic assignment for different traffic demand levels. Results demonstrate that the proposed model produces lower network-wide energy consumption levels compared to traditional energy-efficient and travel time user-optimum traffic assignment methods for both conventional fuel and electric vehicles. Conventional fuel savings relative to travel time routing decrease with increasing traffic demand levels, while electric power savings do not vary monotonically with congestion levels. Energy savings relative to traditional eco-routing are also demonstrated to not vary monotonically with demand levels. Results

*Corresponding Author
Email address: hrakha@vt.edu (Hesham A. Rakha)

of the study also demonstrate that the transportation network layout significantly affects the eco-routing system performance. Finally, the feasibility of the proposed model in real-world applications is discussed and presented.

Keywords: Eco-routing, Microscopic Simulation, Real-time On-board Navigation, Intelligent Transportation Systems, Connected Vehicles, Energy Consumption, Greenhouse Gas Emissions, Route Choice

1. Introduction

On-board navigation, one of the major successful intelligent transportation system (ITS) applications, has been widely used to route vehicles in the most efficient manner. The majority of navigation tools primarily offer the route that provides the shortest distance or minimum travel time, and cannot guarantee the optimum in terms of energy consumption. For example, the shortest distance route, although it minimizes the vehicle miles traveled (VMT), may result in more energy use per unit distance if congestion occurs on the route. Likewise, vehicles running on the faster route may generate higher energy and emission levels given higher travel speeds. Furthermore, there may be cases where travel time-based routing requires traveling longer distances, resulting in higher fuel consumption and emission levels Ahn and Rakha (2008). To improve environmental sustainability from the route planning perspective, an innovative routing concept, known as eco-routing, has been recently proposed Ericsson et al. (2006); Barth et al. (2007) in response to rising energy costs and increasing environmental concerns.

Vehicle energy consumption and emissions depend on numerous factors, including traffic conditions (e.g. speed, acceleration, congestion level), road attributes (e.g. road type and vertical grade), and vehicle characteristics (e.g. vehicle type and weight). The majority of the state-of-the-art eco-routing models, however, cannot incorporate these factors in a single link cost function. An early study Tzeng and Chen (1993) developed a macroscopic traffic assignment model and investigated various solutions that minimized carbon monoxide (CO) emissions constrained by other factors such as travel time and distance. The model assumed that road link emission costs were a constant for a specific link, and thus did not capture variations in emissions associated with traffic operational conditions, vehicle type and road characteristics. The assumption of constant link-specific cost factors was also applied in Nagurney et al.'s study Nagurney (2000); Nagurney and Dong (2002), which developed a multi-class and multi-criteria traffic network equilibrium model with an environmental criterion.

Alternatively, some researchers considered average vehicle operating conditions while estimating link cost functions. For example, Rilett et al. Rilett and Benedek (1994);

Benedek and Rilett (1998) proposed a traffic assignment system that considered User Equilibrium (UE) and System Optimum (SO) traffic assignment in which the objective was to minimize CO emissions. The link cost was modeled as a function of the link average speed. The system outperformed Tzeng's model by considering the variation in emissions as a function of average speed. Another macroscopic model was developed by Sugawara and Niemeier Sugawara and Niemeier (2002), which also used average speed CO emission factors to generate routing solutions. The results of the study demonstrated that emission-optimized trip assignments could reduce system-level vehicle emissions moderately compared to time-dependent UE and SO solutions, and were most effective when the network experienced low to moderately congested conditions. It was also found that less traffic was assigned to freeway routes for the emission assignment given that vehicles produced significantly more emissions when traveling at high speeds. Other studies, such as Chen et al. (2011); Chen and Yang (2012); Li et al. (2013), also characterized environmental measures based on link- or area-aggregated parameters.

The aforementioned macroscopic models are unable to capture differences in environmental measures associated with transient vehicle operation, vehicle and road attribute effects, which have been demonstrated to significantly impact vehicle fuel consumption and emission levels (Ahn et al. (2002); Rakha et al. (2004a)). Consequently, these models are not suitable for operational level analysis such as evaluating the energy and environmental impacts of ITS deployments.

Other eco-routing methods were developed at either mesoscopic or microscopic levels. For example, Barth et al. (2007); Boriboonsomsin et al. (2012); Li et al. (2018) proposed an eco-routing navigation system that combined a microscopic energy/emissions model (CMEM, comprehensive modal emissions model) with a large vehicle activity database to create functional relationships between link-based energy/emission factors and a set of link-based explanatory variables (e.g. speed and road grade). The built-in link cost function, however, formulated fuel consumption and emissions based on the average link speed and grade without considering their transient spatio-temporal variations along the link. Ignoring these microscopic elements has been demonstrated to result in incorrect routing solutions Ahn and Rakha (2008). Furthermore, the model does not provide vehicle-specific routing recommendations.

Nie and Li (2013) incorporated some microscopic factors (e.g. between-link acceleration and idling delay) into their eco-routing model. The model basically assumed that vehicles accelerated/decelerated only when they were traveling from one link to another, ignoring the within-link speed variation. The model also fails to address the variation of environmental measures associated with road grade and does not provide vehicle-specific cost functions.

Rakha et al. (2012) developed a novel agent-based eco-routing system within a sim-

ulation environment, known as the ECO-Agent Feedback Assignment (ECO-AFA) that, unlike previous approaches, captures and uses dynamic transient behavior to estimate instantaneous vehicle fuel consumption levels. These instantaneous estimates are then accumulated to compute link-level costs. The system is able to dynamically update the link cost and route vehicles using the latest real-time information to generate an incremental user-optimal traffic assignment. The optimum route for a specific vehicle is computed at the time of departure of that vehicle from its origin and from each link along its trip to its destination, ensuring that the path computation is based on the most recent information available at that time. This approach fuses the resulting fuel consumption from different vehicles to compute the link cost that is used to route all vehicle types. This model, like all the previously described models, is unable to customize the route recommendations to specific vehicle types. This model was enhanced in Elbery et al. (2016) by adopting an ant-colony based updating methodology to automatically update the link costs when vehicles are stuck on a link due to severe congestion. Further extensions to the model entailed extending the model to compute the system optimum traffic assignment Elbery and Rakha (2017). Several recent studies Rakha et al. (2011); Edwardes and Rakha (2014); Wu et al. (2014a) have demonstrated that the optimum fuel economy cruise speed varies as a function of the vehicle type, implying that eco-routes may differ.

Some researchers have provided valuable insights into electric vehicle eco-routing. For example, Masikos et al. (2014, 2015) proposed an approach to determine the most energy efficient route for electric vehicles based on a mesoscopic energy consumption model. Liu et al. (2014) formulated a joint charging and routing optimization problem for electric vehicle navigation systems. The study calculated link energy consumption based on the link length and travel time, which failed to model transient vehicle behavior. Another study by De Nunzio et al. (2017) considered the impact of between-link acceleration on routing solutions without capturing within-link transient behavior. Other studies considered either plug-in or hybrid electric vehicle eco-routing Yi and Bauer (2018); Qi et al. (2018); De Nunzio et al. (2018); Yi et al. (2018); Houshmand and Cassandras (2018); Fiori et al. (2019); Shen et al. (2019). Most of these studies, however, assume electric vehicles as a standalone entity, ignoring their interplay with conventional vehicles and the impact of real-time traffic conditions on routing solutions. Also, those research findings provide inadequate insights into the routing solutions associated with instantaneous vehicle motion, regenerative braking, and vehicle type.

In summary, apart from Rakha et al. (2012); Elbery et al. (2016), existing eco-routing research efforts fail to use cost functions that capture all transient vehicle behavior along a link. Furthermore, all existing research efforts are unable to tailor routes to specific vehicle types using the same data collected from all vehicles. This paper attempts to address this research need modeling both conventional gasoline/diesel and electric vehicles. It

should be noted that the major goal of this paper is to reduce vehicle energy consumption through optimizing vehicle routing. The proposed eco-routing model is the first effort to develop a vehicle-agnostic link cost function that can be used to compute vehicle-specific energy-optimum routes. The proposed model is incorporated in a microsimulation framework to quantify the network-wide impacts of the proposed dynamic energy-efficient user-equilibrium traffic assignment that is based on the proposed vehicle-agnostic link-specific variables.

The rest of the paper proceeds as follows. Section 3 introduces the modeling background of the study. Section 4 develops the proposed eco-routing model, followed by a numerical testing in Section 5. Section 6 integrates the eco-routing model into a microsimulation framework, and evaluates the network-wide impacts of the model implementation. Section 7 discusses the feasibility of the model in real-world applications. Finally, Sections 8 and 9 provide the concluding remarks of the study and several recommendations for further research.

2. Research contribution

The research presented in this paper is the first attempt to develop a vehicle-agnostic link cost function that retains all transient behavior along the link and is used to compute real-time vehicle-specific energy-optimum routes. The research novelty entails developing a unique vehicle-agnostic approach that allows for the capturing of transient data from all connected vehicles (regardless of their type) in real-time for use in assigning traffic in a energy-efficient manner. The eight variables that are gathered are vehicle agnostic and can be used in conjunction with vehicle parameters to compute vehicle-specific link costs that capture all transient behavior along a link (including regenerative braking) and thus not sacrificing in model accuracy. We integrate both conventional and electric vehicles into one model and implement the model in a simulation environment to achieve a fuel-optimum dynamic user-equilibrium assignment, which allows us to investigate routing differences and interactions between gasoline/diesel and electric vehicles and also enables vehicles to re-route en-route in real-time.

3. Modeling background

The approach to modeling the eco-routing problem in this paper is built on two energy consumption models: the Virginia Tech Comprehensive Power-based Fuel consumption Model (VT-CPFM) and Electric energy consumption Model (VT-CPEM). The VT-CPFM model is used to model conventional gasoline/diesel vehicles, while the VT-CPEM is developed to predict electric vehicle energy consumption.

3.1. VT-CPFM model

Rakha et al. (2011) developed two Virginia Tech Comprehensive Power-based Fuel consumption Model (VT-CPFM) models (VT-CPFM-1 and VT-CPFM-2) each of which is a two-regime model and characterizes fuel consumption as a second-order polynomial function of vehicle power. The use of a second-order model ensures that a bang-bang control[1] does not result from the application of the model. Furthermore, a higher-order model cannot be calibrated using publicly available data[2]. Consequently, a second-order model achieves a good trade-off between model accuracy and applicability. In this study, only VT-CPFM-1 is utilized given that VT-CPFM-2 requires engine gear data for model calibration and implementation, which is usually not available. The VT-CPFM hereinafter refers to the VT-CPFM-1 model.

The modeling framework is illustrated in Eq. (1) with P the vehicle power at the vehicle wheels (kW) and α_0, α_1, and α_2 the vehicle type-specific model coefficients. The model has been validated for LDVs (Rakha et al. (2011); Park et al. (2013)), diesel and hybrid buses (Wang and Rakha (2016a,c, 2017a)), and heavy duty trucks (Wang and Rakha (2016b, 2017c)), demonstrating a good model fit to field measurements.

$$FC(t) = \begin{cases} \alpha_0 + \alpha_1 P(t) + \alpha_2 P(t)^2, & \forall P(t) \geq 0 \\ \alpha_0, & \forall P(t) < 0 \end{cases} \tag{1}$$

Vehicle power is computed using Eq. (2). In this equation, given that the road incline angle is typically very small, the $\cos(\theta)$ term is not included and the $\sin(\theta)$ term is replaced with $\tan(\theta)$ with minimum loss of accuracy.

$$P(t) = \left(ma(t) + mg\frac{C_r}{1000}(c_1 v(t) + c_2) + 0.5\rho_a A_f C_D v^2(t) + mg \cdot \tan(\theta) \right) \frac{v(t)}{1000\eta_d} \tag{2}$$

where m is the vehicle mass in kg, a is the acceleration level in m/s^2, g is the gravitational acceleration, which equals 9.8066 m/s^2, θ is the road grade angle, C_r, c_1 and c_2 are rolling coefficients (unitless), v is the vehicle speed in m/s, ρ_a is the air density at sea level (1.2256 kg/m^3), A_f is the vehicle frontal area (m^2), C_D is the drag coefficient (unitless), and η_d is the driveline efficiency.

[1] A bang-bang control may arise when the partial derivative of fuel consumption with respect to the vehicle power is not a function of the control variable producing a control strategy that is either full throttle or full braking, which is unrealistic (Saerens et al. (2010); Rakha et al. (2011).)

[2] The VT-CPFM model can be calibrated using the EPA fuel economy ratings for highway and city drive cycles

For more details on the VT-CPFM modeling framework, the reader is referred to Rakha et al. (2011); Wang and Rakha (2017c).

3.2. VT-CPEM model

Fiori et al. (2016) extended the VT-CPFM to develop backward microscopic energy consumption model for electric vehicles, known as VT-CPEM. The model considers instantaneous speed/acceleration, vehicle specification and road gradient as the explanatory variables of electric power, as formulated in Eq.(3):

$$EC(t) = \begin{cases} \frac{P(t)}{\eta_{EM}}, & \forall P(t) \geq 0 \\ P(t) \times \eta_{re}(t), & \forall P(t) < 0 \end{cases} \tag{3}$$

where EC is the electric power consumption in $kW \cdot s$, η_{EM} is the efficiency of the electric motor (91% as suggested by Fiori et al. (2016)), and η_{re} is the regenerative efficiency, which determines the amount of energy recovered during regenerative braking, and is modeled using an exponential function of the vehicle deceleration level, as demonstrated in Eq. (4) with α the model coefficient (0.0411 is used according to the calibration results in Fiori et al. (2016)). Other parameters are defined as before.

$$\eta_{re}(t) = \begin{cases} \frac{1}{e^{\frac{\alpha}{|a(t)|}}}, & \forall P(t) < 0 \\ 0, & \forall P(t) \geq 0 \end{cases} \tag{4}$$

For the positive power condition, the energy flows from the electric motor to the wheels and the power is consumed in the traction mode. Alternatively, in the regenerative braking mode, the energy flows from the wheels back to the motor and is negative, and a portion of the braking power is used to charge the battery.

The model has been tested for light duty vehicles and metro trains, demonstrating a good match between model estimates and field observations. For details of the modeling effort, the reader is referred to Fiori et al. (2016) and Wang and Rakha (2017b).

4. Eco-routing modeling

The key to the proposed eco-routing method is to determine which on-road link information should be retained and used to estimate vehicle-specific link energy costs in real time. The retained information should capture all transient behavior on the link and should also be updated from all vehicle link departures (no matter what type of vehicle traverses the link) to ensure the timeliness of the information. Consequently, the information used should be vehicle-agnostic.

4.1. Link cost function

Our approach to estimating link cost factors is built on the VT-CPFM and VT-CPEM modeling approaches given their robust and previously validated energy estimates and their easy implementation in complex systems. A variant of the models is generated for the link cost formulation purpose, as illustrated in Eqs. (5) and (6). The VSP in the models is the vehicle specific power referring to the power per unit mass of the vehicle (kW/ton). Namely, $VSP(t) = \frac{P(t)}{m/1000}$, where m is in kg.

$$FC(t) = \begin{cases} \alpha_0 + \alpha_1 \frac{m}{1000} VSP(t) + \alpha_2 \left(\frac{m}{1000} VSP(t) \right)^2, & \forall VSP(t) \geq 0 \\ \alpha_0, & \forall VSP(t) < 0 \end{cases} \tag{5}$$

$$EC(t) = \begin{cases} \frac{m}{1000} \frac{VSP(t)}{\eta_{EM}}, & \forall VSP(t) \geq 0 \\ \frac{m}{1000} VSP(t) \eta_{re}(t), & \forall VSP(t) < 0 \end{cases} \tag{6}$$

Eqs. (5) and (6) estimate energy consumption at an instantaneous level. The link-aggregated energy cost is thus calculated by accumulating the instantaneous model estimates, as illustrated in Eqs. (7) and (8):

$$FC_l = TT \times \alpha_0 + \alpha_1 \frac{m}{1000} \sum_t VSP^{(+)}(t) + \alpha_2 \left(\frac{m}{1000} \right)^2 \sum_t VSP^{2(+)}(t) \tag{7}$$

$$EC_l = \frac{m}{1000 \eta_{EM}} \left(\sum_t VSP^{(+)}(t) \right) + \frac{m}{1000} \sum_t \left((VSP^{(-)}(t) \times \eta_{re}(t) \right) \tag{8}$$

where FC_l and EC_l are link-level conventional fuel (l) and electric power (Wh) consumption, respectively; TT is the link travel time (s); $VSP^{(+)}$ and $VSP^{(-)}$ are the positive and negative vehicle specific powers, respectively; and $VSP^{2(+)}$ is the power square for the positive power. Four link-based parameters are generated based on the equations: TT, $\sum_t VSP^{(+)}(t)$, $\sum_t VSP^{2(+)}(t)$, and $\sum_t (VSP^{(-)}(t) \times \eta_{re}(t))$. Unlike link average speed, the VSP-based link variables capture all transient behavior along a link given that the VSP generated by the engine is a function of the forces acting on a vehicle including the aerodynamic, rolling, grade and acceleration forces that instantaneously capture traffic conditions, road attributes, vehicle specifications and the interactions between them.

Nonetheless, VSP, like energy consumption, also varies with vehicle type. For the same traffic operational conditions, different vehicle types may require different levels of

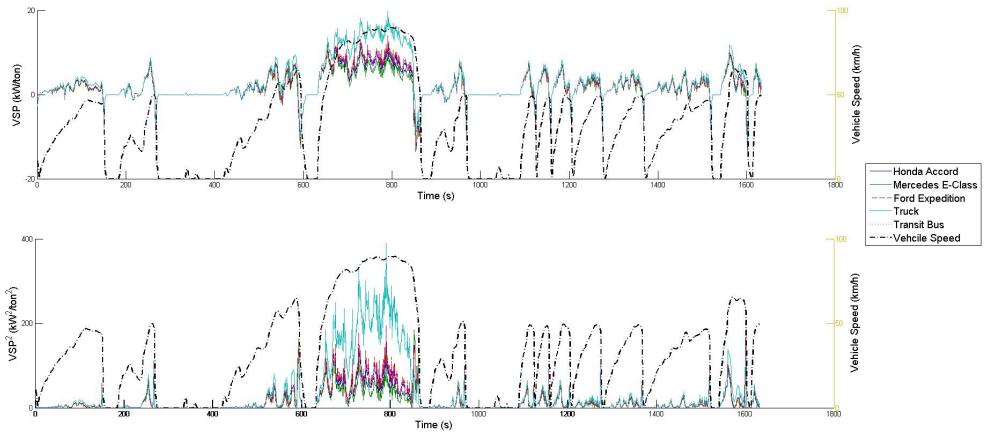

Fig. 1: Comparison of vehicle power between vehicle models

power to overcome their resistance forces and move forward. To illustrate this fact, a test was conducted for different vehicle models on an identical drive cycle. Fig.1 demonstrates that a truck exerts significantly higher VSP levels than the other tested vehicles, especially at high speeds. That is because of the higher aerodynamic resistance force. The tested Mercedes passenger car exerts the lowest level of power given its small aerodynamic resistant force. Consequently, VSP is vehicle type specific, and the three link-specific VSP-based parameters ($\sum_t VSP^{(+)}(t)$, $\sum_t VSP^{2(+)}(t)$, and $\sum_t (VSP^{(-)}(t) \times \eta_{re}(t))$) produce significant errors in the link-level vehicle power exerted by different vehicle types. Consequently, a better set of variables is needed to capture vehicle transient behavior.

Generating robust routing solutions in real-time is essential to on-board navigation applications. In addition to considering microscopic elements, it is important to identify the link-based variables that are not affected by vehicle type and thus can be shared in real-time to calculate link energy cost factors. As mentioned earlier, VSP equals the actual power divided by the vehicle mass and consists of four components: 1. the power to overcome the rolling resistance ($g \cdot \frac{C_r}{1000}(c_1 v(t) + c_2) \times \frac{v(t)}{\eta_d}$); 2. the power to overcome the grade resistance ($g \cdot \tan(\theta) \times \frac{v(t)}{\eta_d}$); 3. the power exerted to accelerate the vehicle ($\frac{a(t)v(t)}{\eta_d}$); and 4. the power to overcome the aerodynamic resistance ($0.5\rho_a \frac{A_f C_D}{m} v^2(t) \times \frac{v(t)}{\eta_d}$). The summation of the first three components of the VSP function, denoted as VSP_{rga}, is vehicle independent. Specifically, gravitational acceleration (g) is a constant relative to a specific geographical location. Road grade (θ) depends on the terrain of the road network. The rolling coefficients (C_r, c_1 and c_2) are determined by pavement type and vehicle tire specifications, which could be assumed to be a constant for the majority of the vehicle

fleet. Speed (v) and acceleration (a) depend on traffic conditions, and driveline efficiency (η_d) is also assumed to be a constant for most vehicle models (0.9 is suggested in the literature Fitch (1993); Rakha et al. (2001, 2011); Fiori et al. (2016)). In the fourth component, $\frac{A_f C_D}{m}$ is determined by vehicle type. ρ_a is the air density is only affected by the air pressure of the test location (1.2256 kg/m^3 at sea level at a temperature of 25 °C). For simplicity, VSP is re-formulated as demonstrated in Eq.(9) in which VSP is separated into two components: VSP_{rga} and $0.5\frac{\rho_a}{\eta_d}\frac{A_f C_D}{m} \cdot v^3(t)$.

$$VSP(t) = VSP_{rga}(t) + 0.5\frac{\rho_a}{\eta_d}\frac{A_f C_D}{m} \cdot v^3(t) \tag{9}$$

Substituting Eq.(9) into Eqs.(7) and (8), the three VSP-based parameters are re-formulated as demonstrated in Eqs.(10)-(12) with $(+)$ and $(-)$ the positive and negative power conditions, respectively. Seven link-based variables independent of vehicle type are identified in Eqs.(10)-(12): $\sum_t v^3(t)^{(+)}$, $\sum_t v^6(t)^{(+)}$, $\sum_t VSP_{rga}^{(+)}(t)$, $\sum_t VSP_{rga}^{2(+)}(t)$, $\sum_t(VSP_{rga}^{(+)}(t) \cdot v^3(t)^{(+)})$, $\sum_t(VSP_{rga}^{(-)}(t) \cdot \eta_{re}(t))$, $\sum_t(v^3(t)^{(-)} \cdot \eta_{re}(t))$. These variables as well as the link travel time (TT), namely, a total of eight variables that are independent of vehicle specifications can be dynamically updated and shared across all vehicles, and thus are suitable for real-time applications.

$$\sum_t VSP^{(+)}(t) = \sum_t VSP_{rga}^{(+)}(t) + 0.5\frac{\rho_a}{\eta_d}\frac{A_f C_D}{m} \cdot \sum_t v^3(t)^{(+)} \tag{10}$$

$$\begin{aligned}
\sum_t VSP^{2(+)}(t) &= \sum_t \left(VSP_{rga}^{(+)}(t) + 0.5\frac{\rho_a}{\eta_d}\frac{A_f C_D}{m} \cdot v^3(t)^{(+)} \right)^2 \\
&= \sum_t \left[VSP_{rga}^{2(+)}(t) + \left(0.5\frac{\rho_a}{\eta_d}\frac{A_f C_D}{m} \right)^2 \cdot v^6(t)^{(+)} \right. \\
&\left. + \frac{\rho_a}{\eta_d}\frac{A_f C_D}{m} \cdot VSP_{rga}^{(+)}(t) \cdot v^3(t)^{(+)} \right] \\
&= \sum_t VSP_{rga}^{2(+)}(t) + \left(0.5\frac{\rho_a}{\eta_d}\frac{A_f C_D}{m} \right)^2 \cdot \sum_t v^6(t)^{(+)} \\
&+ \frac{\rho_a}{\eta_d}\frac{A_f C_D}{m} \cdot \sum_t \left(VSP_{rga}^{(+)}(t) \cdot v^3(t)^{(+)} \right)
\end{aligned} \tag{11}$$

$$\sum_t (VSP^{(-)}(t) \times \eta_{re}(t)) = \sum_t \left[\left(VSP^{(-)}_{rga}(t) + 0.5 \frac{\rho_a}{\eta_d} \frac{A_f C_D}{m} \cdot v^3(t)^{(-)} \right) \cdot \eta_{re}(t) \right]$$
$$= \sum_t \left(VSP^{(-)}_{rga}(t) \cdot \eta_{re}(t) \right) + 0.5 \frac{\rho_a}{\eta_d} \frac{A_f C_D}{m} \cdot \sum_t \left(v^3(t)^{(-)} \cdot \eta_{re}(t) \right) \tag{12}$$

Rather than using average speed; instead the eight variables are computed for each link and shared with vehicles for use with the vehicle parameters to estimate vehicle-specific energy cost factors. The resulting link cost functions are presented in Eqs. (13) and (14), where $(\cdot)_p$ represents the parameters for vehicle model p, and $(\cdot)_l$ refers to the parameters specific to link l; $FC_{l,p}$ and $EC_{l,p}$ are the aggregated conventional fuel and electric energy costs for vehicle model p on link l. The use of the eight variables enables the link cost factors and eco-routes to be updated based on the most recent information gathered by all vehicles and simultaneously generates realistic eco-routing suggestions that are vehicle- and engine-specific.

$$FC_{l,p} = TT_l \times \alpha_{0,p} + \alpha_{1,p} \frac{m_p}{1000} \left[\left(\sum_t VSP^{(+)}_{rga}(t) \right)_l + 0.5 \frac{\rho_{air}}{\eta_d} \frac{A_{f,p} C_{D,p}}{m_p} \cdot \left(\sum_t v^3(t)^{(+)} \right)_l \right]$$
$$+ \alpha_{2,p} (\frac{m_p}{1000})^2 \left[\left(\sum_t VSP^{2(+)}_{rga}(t) \right)_l + \left(0.5 \frac{\rho_{air}}{\eta_d} \frac{A_{f,p} C_{D,p}}{m_p} \right)^2 \cdot \left(\sum_t v^6(t)^{(+)} \right)_l \right.$$
$$\left. + \frac{\rho_{air}}{\eta_d} \frac{A_{f,p} C_{D,p}}{m_p} \cdot \left(\sum_t (VSP^{(+)}_{rga}(t) \cdot v^3(t)^{(+)}) \right)_l \right] \tag{13}$$

$$EC_{l,p} = \frac{m_p}{1000 \eta_{EM}} \left[\left(\sum_t VSP^{(+)}_{rga}(t) \right)_l + 0.5 \frac{\rho_{air}}{\eta_d} \frac{A_{f,p} C_{D,p}}{m_p} \cdot \left(\sum_t v^3(t)^{(+)} \right)_l \right]$$
$$+ \frac{m_p}{1000} \left[\left(\sum_t (VSP^{(-)}_{rga}(t) \cdot \eta_{re}(t)) \right)_l + 0.5 \frac{\rho_{air}}{\eta_d} \frac{A_{f,p} C_{D,p}}{m_p} \cdot \left(\sum_t (v^3(t)^{(-)} \cdot \eta_{re}(t)) \right)_l \right] \tag{14}$$

4.2. Eco-routing formulation

With the developed link cost functions, the formulation of the eco-routing problem is presented in this section. Consider a network G($\mathscr{N}$,$\mathscr{L}$, $\mathscr{P}$) that consists of a set of nodes

$\mathscr{N}$ and a set of links $\mathscr{L}$, assuming that there are $\mathscr{P}$ vehicle types in the network. The objective of the proposed eco-routing problem is to minimize the trip energy consumption for each vehicle traveling from origin (O) to destination (D), as demonstrated in Eq.(15).

$$Min\ Z = \sum_{i,j\in\mathscr{N},p\in\mathscr{P}} \Big(FC_{ij,p} y_p + EC_{ij,p}(1-y_p) \Big) x_{i,j} \tag{15a}$$

$$subject\ to: \sum_{j\in\mathscr{N}} x_{i,j} - \sum_{j\in\mathscr{N}} x_{j,i} = \begin{cases} 1, & i = s \\ -1, & i = d, \forall i \in \mathscr{N} \\ 0, & otherwise \end{cases} \tag{15b}$$

$$\eta_{re}(t) = \begin{cases} \frac{1}{e^{\frac{0.0411}{|a(t)|}}}, & \forall P(t) < 0 \\ 0, & \forall P(t) \geq 0 \end{cases} \tag{15c}$$

$$|a(t)| \leq 6 \tag{15d}$$

$$y_p \in (0,1), \forall p \in \mathscr{P} \tag{15e}$$

$$x_{i,j} \in (0,1), \forall i,j \in \mathscr{N} \tag{15f}$$

In this formulation, x_{ij} are the decision variables that determine the selected links by the incoming routing decision. $FC_{ij,p}$ and $EC_{ij,p}$ are link fuel and energy cost factors to travel from node i to j for vehicle type p, which are estimated using Eqs. (13) and (14). Constraint (15b); in which s and d are the origin and destination nodes, respectively; is the link flow conservation equation. Constraint (15c) ensures that energy regeneration only occurs during braking ($P < 0$). Constraint (15d) limits the deceleration level to within 6 m/s^2 to ensure realistic deceleration behavior. Constraints (15e) and (15f) ensure that the vehicle type identifier y_p and the decision variables x_{ij} are dummy variables, respectively.

The proposed model captures the impacts of vehicle type, vehicle transient behavior and the timeliness of road information on routing solutions. It also considers both conventional and electric vehicles, and enables the network-wide evaluation of their routing solutions and interactions. To the best of our knowledge, instantaneous regenerative braking is, for the first time, accounted for in eco-routing. This approach ensures that the optimum routes are tailored for each vehicle type; meaning that vehicles of different types may be assigned different routes.

5. Numerical experiments

A numerical experiment was designed to quantify differences in link/path energy costs and its impact on routing results for the proposed eco-routing method versus traditional

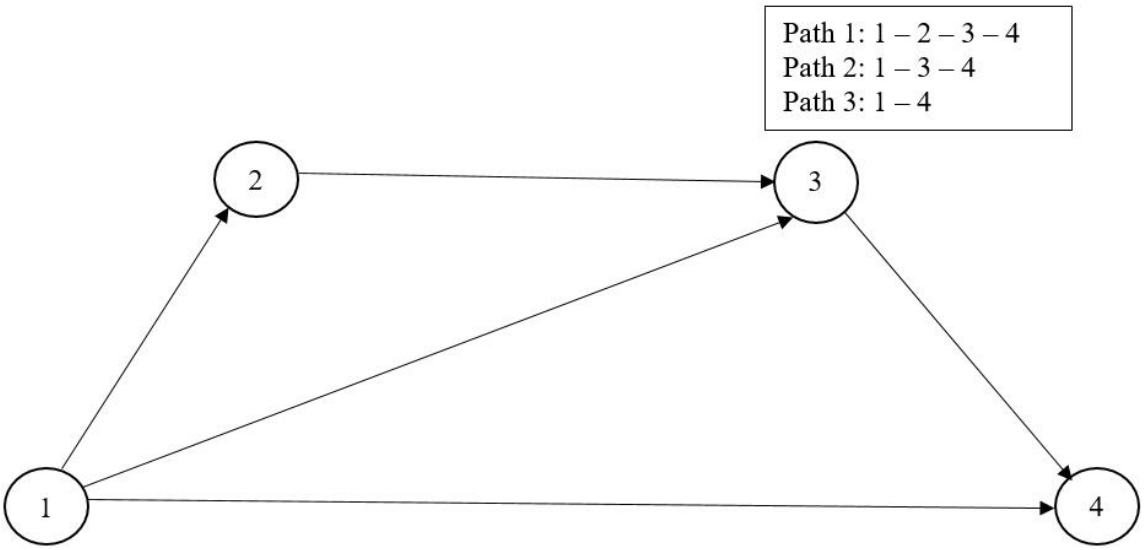

Fig. 2: The configuration of the testing network

methods to quantitatively verify the importance of considering a dynamic vehicle-specific stochastic incremental traffic assignment. The Dijkstras shortest path algorithm Dijkstra (1959) was used to compute the minimum path for the model in Eq.(15). The results demonstrate that traditional methods have limitations in generating robust eco-routing solutions.

5.1. Network Configuration

A sample network composed of four nodes and five links was constructed, as illustrated in Fig.2. Each node refers to a location where vehicles depart or arrive. Each of the links represents a roadway with all the roadways being one-way streets. All traffic is assumed to travel from Node 1 (origin) to Node 4 (destination). No traffic control is considered in order to simplify traffic operational conditions in the network.

Table 1 presents the network characteristics. Specifically, all of the links are single-lane roads except for link 5, which has two lanes. Given that there are two links entering node 3, two lanes are assigned for link 5 in order to eliminate bottlenecks within the system. Three of the links (links 1, 4, and 5) have an identical length of 2 km, and link 2 has a length of 4 km, and link 3 is 6 km long. The configuration of the link length ensures an identical distance of 6 km for each path. The network contains three paths. Path 1 (1-2-3-4), consisting of link 1, link 4 and link 5, has a speed limit of 45 km/h, which is typically considered as a local street route. Path 2 (1-3-4), however, conceives an arterial link with a speed limit of 70 km/h followed by a local street link (link 5). Path 3 (1-4),

Table 1: Network characteristics

Link ID	Starting Node	Ending Node	Number of Lanes	Link Length (km)	Speed Limit (km/h)
1	1	2	1	2	45
2	1	3	1	4	70
3	1	4	1	6	100
4	2	3	1	2	45
5	3	4	2	2	45

Table 2: Specifications of the test vehicles

Vehicle Model	Mass (kg)	Nominal power (kW)	C_D	A_f	C_r	c_1	c_2
Honda Accord	1469	138	0.325	2.3	1.75	0.0328	4.575
Mercedes C300	1550	180	0.24	2.2	1.75	0.0328	4.575
Ford Expedition	2626	272	0.41	3.88	1.75	0.0328	4.575
Truck (International/ 9800 SBA)	7239	261	0.78	8.9	1.75	0.0328	4.575
Transit Bus	12864	336	0.78	8.8	1.75	0.0328	4.575
Tesla S	2108	310	0.24	2.67	1.75	0.0328	4.575
BMW i3	1477	80	0.28	2.33	1.75	0.0328	4.575
Nissan Leaf	1297	125	0.29	2.38	1.75	0.0328	4.575

with a speed limit of 100 km/h, is a freeway route. In summary, the network provides three route alternatives: a local street, an arterial route and a freeway route.

5.2. Test Scenario

In order to model roadway traffic, a simulation was conducted on the sample network using the INTEGRATION software. A total of eight vehicle types were loaded on the network, covering a wide range of vehicle powertrains. The specifications of the tested vehicles are provided in Table 2. The Honda Accord and Mercedes C300 are representative of sedan passenger cars, and Ford Expedition is a full size sport utility vehicle (SUV). One of the truck models in the literature Wang and Rakha (2016b) (International/ 9800 SBA) was tested to characterize typical truck fuel consumption behavior. The tested bus was selected from the fleet modeled in Wang and Rakha (2017a). It should be noted that the bus was tested here only for the purpose of demonstrating the ability of the proposed eco-routing model to differentiate between different vehicle types, and not used for on-board eco-navigation applications given that buses typically have fixed routes and cannot be dynamically re-routed. The Tesla S, BMW i3 and Nissan Leaf are three of the most widely used electric vehicles.

A total demand of 6400 veh/h was loaded on the simulation network for the first 1200 s. Each vehicle model shares an equal demand of 800 veh/h. After the simulation

run, the eight link variables experienced by each vehicle exiting a link were calculated based on the simulated trajectory data. For each of the five links, there were multiple sets of eight variables (each vehicle generated a set of eight variables), which were sorted in ascending order according to the departure time from the link. The sorted parameters of each link were then smoothed using an exponential smoothing procedure, as demonstrated in Eq.(16), where α is the smoothing factor, $[\cdot]'_{n,l}$ is the smoothed link variables when vehicle n departs from link l, $[\cdot]'_{n-1,l}$ is the smoothed link variables when vehicle $n-1$ completes running on link l, and $[\cdot]_{n,l}$ is the experienced link variables by vehicle n going through link l. The smoothing procedure is adopted to predict traffic conditions over the next time step. The last set of link-smoothed variables were considered as the most recent information at the end of the simulation run. Assuming that the routing decision is made at that instant in time, the latest eight variables were thus input to the link cost functions, as illustrated in Eqs.(13) and (14) to estimate vehicle type-specific link energy costs.

$$\left[\sum_t VSP_{rga}^{(+)}(t)\right]'_{n,l} = (1-\alpha)\left[\sum_t VSP_{rga}^{(+)}(t)\right]'_{n-1,l} + \alpha\left[\sum_t VSP_{rga}^{(+)}(t)\right]_{n,l} \tag{16a}$$

$$\left[\sum_t v^3(t)^{(+)}\right]'_{n,l} = (1-\alpha)\left[\sum_t v^3(t)^{(+)}\right]'_{n-1,l} + \alpha\left[\sum_t v^3(t)^{(+)}\right]_{n,l} \tag{16b}$$

$$\left[\sum_t VSP_{rga}^{2(+)}(t)\right]'_{n,l} = (1-\alpha)\left[\sum_t VSP_{rga}^{2(+)}(t)\right]'_{n-1,l} + \alpha\left[\sum_t VSP_{rga}^{2(+)}(t)\right]_{n,l} \tag{16c}$$

$$\left[\sum_t VSP_{rga}^{2(+)}(t)\right]'_{n,l} = (1-\alpha)\left[\sum_t VSP_{rga}^{2(+)}(t)\right]'_{n-1,l} + \alpha\left[\sum_t VSP_{rga}^{2(+)}(t)\right]_{n,l} \tag{16d}$$

$$\left[\sum_t (VSP_{rga}^{(-)}(t)\cdot\eta_{re}(t))\right]'_{n,l} = (1-\alpha)\left[\sum_t (VSP_{rga}^{(-)}(t)\cdot\eta_{re}(t))\right]'_{n-1,l} + \alpha\left[\sum_t (VSP_{rga}^{(-)}(t)\cdot\eta_{re}(t))\right]_{n,l} \tag{16e}$$

$$\left[\sum_t (VSP_{rga}^{(-)}(t)\cdot\eta_{re}(t))\right]'_{n,l} = (1-\alpha)\left[\sum_t (VSP_{rga}^{(-)}(t)\cdot\eta_{re}(t))\right]'_{n-1,l} + \alpha\left[\sum_t (VSP_{rga}^{(-)}(t)\cdot\eta_{re}(t))\right]_{n,l} \tag{16f}$$

$$\left[\sum_t (v^3(t)^{(-)}\cdot\eta_{re}(t))\right]'_{n,l} = (1-\alpha)\left[\sum_t (v^3(t)^{(-)}\cdot\eta_{re}(t))\right]'_{n-1,l} + \alpha\left[\sum_t (v^3(t)^{(-)}\cdot\eta_{re}(t))\right]_{n,l} \tag{16g}$$

$$TT'_{n,l} = (1-\alpha)TT'_{n-1,l} + \alpha TT_{n,l} \tag{16h}$$

To quantify the benefits of the proposed eco-routing model, the results were compared to four other routing methods:

1. Scenario I refers to the proposed eco-routing method. The objective function is set to $\sum_{l\in\mathscr{L},p\in\mathscr{P}}\Big(FC_{l,p}x_p + EC_{l,p}(1-x_p)\Big)y_l$, which uses the most recent eight vari-

ables obtained using Eq.(16) to calculate vehicle type-specific energy consumption shortest paths.

2. Scenario II refers to the traditional eco-routing methods that use average link speed to compute the energy consumption. The average speed of each link is updated in real-time and then input to the energy consumption models to generate vehicle type-specific link costs.
3. Scenario III refers to the traditional INTEGRATION eco-routing method that updates the link energy consumption cost in real-time as formulated by $FC'_{n,l} = (1-\alpha)FC'_{n-1,l} + \alpha FC_{n,l}$ or $EC'_{n,l} = (1-\alpha)EC'_{n-1,l} + \alpha EC_{n,l}$, with FC and EC the conventional fuel and electric power consumption as defined before. The objective function is set to $\sum_{l\in\mathscr{L}} FC_l y_l$ for conventional vehicles and $\sum_{l\in\mathscr{L}} EC_l y_l$ for electric vehicles. The method averages link energy consumption experienced by different vehicle types to achieve link-specific energy costs, ignoring the vehicle type impact on the cost factors. This method results in all vehicle types having the same link energy consumption and thus eco-routes.
4. Scenario IV is essentially an extension of Scenario III. The method also averages link energy consumption to achieve real-time link costs. However, it assumes that vehicle-type specific link costs are affected only by the experiences of the vehicles in the same type and not other vehicles. The link cost updating procedure is demonstrated by $FC'_{n_p,p,l} = (1-\alpha)FC'_{n_p-1,p,l} + \alpha FC_{n_p,p,l}$ and $EC'_{n_p,p,l} = (1-\alpha)EC'_{n_p-1,p,l} + \alpha EC_{n_p,p,l}$, where $[\cdot]'_{n_p,p,l}$ is the smoothed link energy cost for vehicle type p when vehicle n_p departs from link l, $[\cdot]'_{n_p-1,p,l}$ is the smoothed link energy cost for vehicle type p when vehicle n_p-1 completes running on link l, and $[\cdot]_{n_p,p,l}$ is the experienced energy cost of vehicle n_p on link l. The method results in routing solutions based vehicle type-specific real-time information.
5. Scenario V refers to the four variables-based approach (TT, $\sum_t VSP^{(+)}(t)$, $\sum_t VSP^{2(+)}(t)$ and $\sum_t (VSP^{(-)}(t) \times \eta_{re}(t))$), which as aforementioned does not consider the impact of vehicle specifications on power behavior. The objective function of this method is also set to $\sum_{l\in\mathscr{L},p\in\mathscr{P}} \Big(FC_{l,p}x_p + EC_{l,p}(1-x_p) \Big) y_l$. The four variables

are updated in real-time as demonstrated in Eq.(17).

$$\left[\sum_t VSP^{(+)}(t)\right]'_{n,l} = (1-\alpha)\left[\sum_t VSP^{(+)}(t)\right]'_{n-1,l} + \alpha\left[\sum_t VSP^{(+)}(t)\right]_{n,l} \tag{17a}$$

$$\left[\sum_t VSP^{2(+)}(t)\right]'_{n,l} = (1-\alpha)\left[\sum_t VSP^{2(+)}(t)\right]'_{n-1,l} + \alpha\left[\sum_t VSP^{2(+)}(t)\right]_{n,l} \tag{17b}$$

$$\left[\sum_t (VSP^{(-)}(t)\cdot\eta_{re}(t))\right]'_{n,l} = (1-\alpha)\left[\sum_t (VSP^{(-)}(t)\cdot\eta_{re}(t))\right]'_{n-1,l} + \alpha\left[\sum_t (VSP^{(-)}(t)\cdot\eta_{re}(t))\right]_{n,l} \tag{17c}$$

$$TT'_{n,l} = (1-\alpha)TT'_{n-1,l} + \alpha TT_{n,l} \tag{17d}$$

5.3. Results Analysis

The resulting link cost factors and eco-routes are compared for the different vehicle types and eco-routing scenarios, as demonstrated in Tables 3-5.

Table 3 demonstrates that, for Scenarios 1, 2, 4 and 5, the link energy cost factors differ for the different vehicle types. For example, for the conventional vehicles, as expected the trucks and buses produce significantly higher fuel consumption levels compared to the LDVs (Honda Accord, Mercedes C300 and Ford Expedition); and for the electric vehicles, the Tesla in general consumes more energy compared to the BMW i3 and Nissan Leaf. Furthermore, the electric power is in Wh units resulting in significantly different numerical values relative to conventional fuel in $liters$. Consequently, Scenario 3 generated energy costs for conventional and electric vehicles, respectively. However, the vehicle types in either cluster of conventional vehicles or the cluster of electric vehicles have the same link cost and cannot be differentiated. For a specific vehicle type, the differences in link cost between Scenario 1 and Scenarios 2, 3, and 5 demonstrate that failing to consider the effects of link transient behavior and vehicle type on either energy consumption or power behavior results in link cost errors. The results of Scenario 4 demonstrate that an estimation bias may also result from failing to capture real-time information.

Table 4 presents the resulting path costs for each of the scenarios. The results demonstrate that, as expected, the costs differ for the different vehicle types and eco-routing scenarios except for Scenario III. In addition, the link cost errors demonstrated in Table 3

Table 3: Link energy cost factors

Link ID	Vehicle Model	Link Energy Cost (Conventional fuel in l, electric power in Wh)				
		Scenario I	Scenario II	Scenario III	Scenario IV	Scenario V
Link 1	Honda Accord	0.129	0.101	0.312	0.125	0.13
	Mercedes C300	0.119	0.097	0.312	0.115	0.122
	Ford Expedition	0.153	0.13	0.312	0.147	0.153
	Truck (International/ 9800 SBA)	0.520	0.509	0.312	0.516	0.490
	Transit Bus (19XX)	0.663	0.659	0.312	0.659	0.671
	Tesla S	154.547	182.401	117.649	162.881	177.198
	BMW i3	116.043	141.929	117.649	116.465	124.156
	Nissan Leaf	106.375	132.780	117.649	109.281	109.025
Link 2	Honda Accord	0.183	0.166	0.475	0.177	0.182
	Mercedes C300	0.182	0.172	0.475	0.179	0.189
	Ford Expedition	0.252	0.259	0.475	0.252	0.241
	Truck (International/ 9800 SBA)	1.066	1.189	0.475	1.091	0.873
	Transit Bus (19XX)	1.379	1.522	0.475	1.400	1.329
	Tesla S	407.844	478.532	366.064	422.723	471.068
	BMW i3	323.31	390.596	366.064	343.146	330.061
	Nissan Leaf	305.562	374.889	366.064	331.348	289.837
Link 3	Honda Accord	0.242	0.260	1.162	0.244	0.246
	Mercedes C300	0.260	0.284	1.162	0.261	0.299
	Ford Expedition	0.437	0.589	1.162	0.454	0.414
	Truck (International/ 9800 SBA)	2.062	2.631	1.162	2.089	1.539
	Transit Bus (19XX)	2.608	3.245	1.162	2.742	2.589
	Tesla S	848.627	1071.620	769.088	854.441	1109.99
	BMW i3	708.914	924.793	769.088	732.037	777.731
	Nissan Leaf	688.441	912.404	769.088	706.085	682.95
Link 4	Honda Accord	0.107	0.101	0.439	0.001	0.110
	Mercedes C300	0.102	0.097	0.439	0.001	0.112
	Ford Expedition	0.134	0.130	0.439	0.135	0.143
	Truck (International/ 9800 SBA)	0.506	0.509	0.439	0.515	0.503
	Transit Bus (19XX)	0.653	0.659	0.439	0.004	0.751
	Tesla S	174.147	182.401	171.696	171.696	253.851
	BMW i3	134.198	141.929	171.696	2.998	177.864
	Nissan Leaf	124.867	132.780	171.696	2.789	156.188
Link 5	Honda Accord	0.082	0.083	0.354	0.082	0.085
	Mercedes C300	0.086	0.086	0.354	0.087	0.1
	Ford Expedition	0.135	0.129	0.354	0.127	0.136
	Truck (International/ 9800 SBA)	0.626	0.593	0.354	0.612	0.51
	Transit Bus (19XX)	0.799	0.760	0.354	0.764	0.844
	Tesla S	254.889	238.634	196.126	229.275	352.266
	BMW i3	209.863	194.699	196.126	198.048	246.820
	Nissan Leaf	202.321	186.829	196.126	186.678	216.741

Table 4: Path energy cost

Vehicle Model	Path ID	Scenario I	Scenario II	Scenario III	Scenario IV	Scenario V
Honda Accord[1]	1	0.3179	0.284	1.1052	0.2076	0.3253
	2	0.2651	0.249	0.8284	0.2589	0.2672
	3	0.2421	0.26	1.1624	0.2439	0.2458
Mercedes C300[1]	1	0.3075	0.281	1.1052	0.2025	0.3348
	2	0.2686	0.258	0.8284	0.266	0.2899
	3	0.2599	0.284	1.1624	0.2611	0.2989
Ford Expedition[1]	1	0.4219	0.389	1.1052	0.4084	0.4314
	2	0.3874	0.388	0.8284	0.3791	0.3772
	3	0.4369	0.589	1.1624	0.4544	0.4138
Truck (International/ 9800 SBA)[1]	1	1.6518	1.612	1.1052	1.643	1.5023
	2	1.6922	1.782	0.8284	1.7031	1.3825
	3	2.0621	2.631	1.1624	2.0888	1.5394
Transit Bus (19XX)[1]	1	2.1152	2.077	1.1052	1.4276	2.2658
	2	2.178	2.282	0.8284	2.164	2.1726
	3	2.6083	3.245	1.1624	2.742	2.5891
Tesla S[2]	1	583.5833	603.435	485.4716	563.8517	783.3154
	2	662.7326	717.166	562.1901	651.9976	823.3346
	3	848.6269	1071.62	769.0876	854.4408	1109.9905
BMW i3[2]	1	460.1037	478.558	485.4716	317.511	548.841
	2	533.173	585.295	562.1901	541.1933	576.8811
	3	708.9137	924.793	769.0876	732.0366	777.7305
Nissan Leaf[2]	1	433.5625	452.389	485.4716	298.747	481.9545
	2	507.8838	561.718	562.1901	518.0252	506.5773
	3	688.4415	912.404	769.0876	706.0848	682.9495

[1]Conventional fuel: l. [2]Electric energy: Wh.

result in differences in path costs between the proposed scenario and the other four scenarios. For example, the Honda Accord fuel consumption on path 1 is 0.3179 l for Scenario I, whereas it is 0.284, 1.1052, 0.2076, and 0.3253 l for Scenarios II, III, IV and V, respectively.

The eco-routes were identified based on the path costs, as illustrated in Table 5. In general, either different vehicle types or eco-routing scenarios may result in different routing solutions. Specifically, according to the results of the proposed model (Scenario I), the Honda Accord and Mercedes C300 (sedan passenger car) are routed along path 3 (freeway route: 1 - 4) to minimize their fuel consumption levels; while the Ford Expedition (SUV) is routed along path 2 (arterial route: 1 - 3 - 4), and the truck and bus (HDVs) as well as the Tesla S, BMW i3 and Nissan Leaf (electric vehicles) are routed along path 1 (local street: 1 - 2 - 3 - 4). The routing results are reasonable, given that the optimum fuel economy cruise speed is approximately 80 km/h for the Honda Accord and Mercedes C300 and 58 km/h for the Ford Expedition, while it ranges between 30 and 50 km/h for HDVs Wang and Rakha (2016a,c,b, 2017a) and 15 to 25 km/h for electric vehicles (Wu et al. (2014b)).

Table 5: Comparison of eco-routes

Vehicle Model	Scenario I		Scenario II		Scenario III		Scenario IV		Scenario V	
	Minimum Path	Minimum cost	Minimum Path	Minimum cost	Minimum Path	Minimum cost	Minimum Path	Minimum cost	Minimum Path	Minimum cost
Honda Accord[1]	1–4	0.2421	1–3–4	0.249	1–3–4	0.8284	1–2–3–4	0.2076	1–4	0.2458
Mercedes C300[1]	1–4	0.2599	1–3–4	0.258	1–3–4	0.8284	1–2–3–4	0.2025	1–3–4	0.2899
Ford Expedition[1]	1–3–4	0.3874	1–3–4	0.388	1–3–4	0.8284	1–3–4	0.3791	1–3–4	0.3772
Truck (International/ 9800 SBA)[1]	1–2–3–4	1.6518	1–2–3–4	1.612	1–3–4	0.8284	1–2–3–4	1.643	1–3–4	1.3825
Transit Bus (19XX)[1]	1–2–3–4	2.1152	1–2–3–4	2.077	1–3–4	0.8284	1–2–3–4	1.4276	1–3–4	2.1726
Tesla S[2]	1–2–3–4	583.5833	1–2–3–4	603.435	1–2–3–4	485.4716	1–2–3–4	563.8517	1–2–3–4	783.3154
BMW i3[2]	1–2–3–4	460.1037	1–2–3–4	478.558	1–2–3–4	485.4716	1–2–3–4	317.511	1–2–3–4	548.841
Nissan Leaf[2]	1–2–3–4	433.5625	1–2–3–4	452.389	1–2–3–4	485.4716	1–2–3–4	298.747	1–2–3–4	481.9545

[1]Conventional fuel: l. [2]Electric energy: Wh.

The tested passenger cars are thus assigned to the freeway route, which results in a speed closer to their optimum cruise speeds; while the arterial route, consisting of two links with speed limits of 70 km/h and 45 km/h, generates a speed closer to the optimum speed for the Ford Expedition. HDVs and electric vehicles, however, are routed along local streets given their significantly lower optimum cruise speeds. It should be noted that, to simplify traffic operations, no traffic control was modeled, and thus, the prevailing speed of each route determines the optimum eco-routing solutions. In reality, however, traffic operations are more complex. The route with the prevailing speed closer to the optimum cruise speed may not always be environmentally better. For example, a route with traffic signals may lead to frequent stop-and-go maneuvers, resulting in significantly higher energy consumption levels.

Compared to the proposed scenario, the other four scenarios generate different routing solutions for some of the vehicle types. Specifically, without considering link transient behavior, Scenario II results in the Honda Accord and Mercedes C300 choosing the arterial route to minimize their fuel consumption levels. Scenario III assigns all conventional vehicles to the arterial route given the inability to differentiate between vehicle types. Scenario IV routes the Honda Accord and Mercedes C300 to the local streets given that the eco-routing logic is not based on real-time information. Scenario V also provides inconsistent results by routing the Mercedes C300, the truck and bus to the arterial route, which results from the fact that the routing model is unable to capture the effect of vehicle specifications on the exerted power.

6. Network-wide eco-routing test

In order to quantify the system-wide benefits of the proposed eco-routing method for typical traffic operations, the model was implemented and tested in the INTEGRATION microscopic simulation software. Unlike the numerical experiment presented earlier, the

simulation test provides a microscopic and macroscopic evaluation of the proposed eco-routing system.

6.1. Background of the simulation framework

The applicability of a simulation software to eco-routing highly depends on the accuracy of the resulting vehicle trajectories and built-in energy consumption models. A suitable simulation model should be able to adequately characterize realistic vehicle motion and energy consumption behavior. In addition, the simulation testbed is also expected to easily model large transportation networks and simultaneously assign traffic dynamically.

INTEGRATION, an agent-based microscopic traffic assignment and simulation software Van Aerde and Yagar (1988); Van Aerde and Rakha (2007); Rakha (2002), conceives an integrated simulation and traffic assignment model and performs traffic simulations by tracking the movement of individual vehicles every deci-second Rakha et al. (2012). The built-in car following model (Rakha-Pasumarthy-Adjerid car following model) has been demonstrated to adequately capture both steady-state Van Aerde (1995); Van Aerde and Rakha (1995) and non-steady-state car following behavior Rakha et al. (2001, 2004b). INTEGRATION also offers robust lane changing logic by considering both mandatory and discretionary lane changing Rakha and Zhang (2004, 2006). It is worth noting that a buffer is offered in INTEGRATION for the mandatory lane changing to avoid congestion that would occur if all drivers make lane changes at the same location to abandon the current lane to move forward, adequately capturing the heterogeneity of lane changing behavior in reality. Furthermore, a recent study has demonstrated that INTEGRATION is able to generate realistic VSP distributions and accurate energy predictions Wang et al. (2017) given the robust built-in car following model and energy consumption models (VT-CPFM and VT-CPEM). Consequently, INTEGRATION is selected as the simulation tool for the proposed study.

In the INTEGRATION framework, the selection of the next link to be taken by a vehicle is determined by the model's internal routing logic Rilett et al. (1991); Rilett and Van Aerde (1991). Before this study, there were 10 built-in routing methods in INTEGRATION:

1. Time-Dependent Method of Successive Averages (MSA)
2. Time-Dependent Sub-Population Feedback Assignment (SFA)
3. Time-Dependent Agent Feedback Assignment (AFA)
4. Time-Dependent Dynamic Traffic Assignment (DTA)
5. Time-Dependent Frank-Wolf Algorithm (FWA)
6. Time-Dependent External Routing 1 File 8 (ER1)
7. Time-Dependent External Routing 2 File 9 (ER2)

8. Distance Based Routing
9. ECO-Subpopulation Feedback Assignment (ECO-SFA)
10. ECO-Agent Feedback Assignment (ECO-AFA)

Some of these methods are static and deterministic (i.e. MSA, FWA, Distance Based Routing), while some are dynamic and stochastic (i.e. SFA, AFA, ECO-SFA, ECO-AFA). Regardless of the particular method used to route vehicles, the selection of the next link that a vehicle should take is done using a vehicle-specific array that lists for the vehicle the entire sequence of links from its origin to its destination. Upon the completion of any link, a vehicle simply queries this array to determine which link it should utilize next to reach its ultimate destination in the most efficient manner. When travel across this next link is in turn completed, the selection process is then repeated until a link whose downstream node is the vehicle's final trip destination Rakha et al. (2012).

Among these routing options, ECO-SFA and ECO-AFA are the eco-routing algorithms that are able to dynamically compute eco-routes based on the feedback link fuel costs experienced by the vehicles departing from each link. Specifically, ECO-SFA is a sub-population-based routing logic that equally divides all routing vehicles into five sub-populations. The minimum paths for each of the five sub-populations are computed by every user-specified time interval, demonstrating that path computation may often be several seconds or minutes old and thus not based on the most recent information. Alternatively, ECO-AFA assigns vehicles individually. Link costs and eco-routes are computed upon each vehicle's departure from a link, rather than by average time interval. The agent-based routing logic enables eco-routing using the most recent information. However, neither the ECO-AFA algorithm nor the ECO-SFA are able to generate vehicle type-specific eco-routes. The proposed eco-routing system was developed to address this gap.

6.2. Dynamic eco-routing system

In this section, the proposed eco-routing model is implemented in the INTEGRATION framework and thus extended to the incremental dynamic traffic assignment model. It should be noted that the optimal solutions are solved using INTEGRATION's existing routing logic (Dijkstras algorithm Dijkstra (1959)); however, the proposed eco-routing model may generate different solutions given that is accounts for the vehicle specifications when computing its routes. The general architecture of the simulation-based eco-routing system is presented in Fig.3.

The system requires the input of road characteristics, signal information, origin-destination (OD) demands and vehicle specifications. The routing logic starts from an initialization procedure in which routes are selected based on the energy consumption estimated using the facility's free-flow speed. The use of free-flow speed is attributed to the fact that the

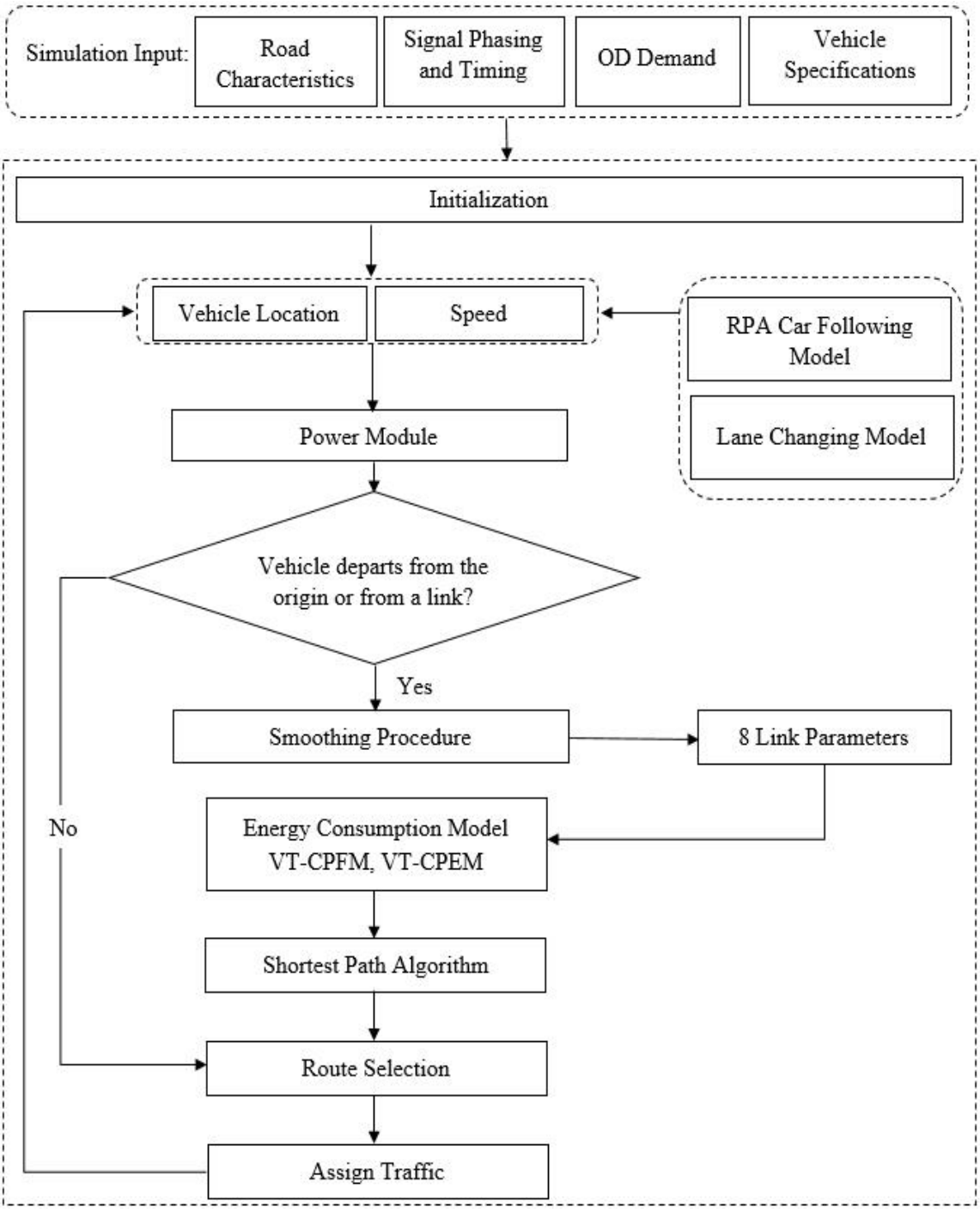

Fig. 3: INTEGRATION framework for the dynamic eco-routing system

network is initially empty. Once the route is selected, INTEGRATION updates the vehicle longitudinal and lateral motion every deci-second using the built-in RPA car-following model and a lane-changing model. The vehicle locations and speeds are recorded on an instantaneous basis and used to compute the cumulative eight variables. Once a vehicle completes a link, the link aggregated eight variables are sent to the cloud and fused with the experiences of other vehicles using an exponential smoothing procedure, as demonstrated in Equation (16), where α is the smoothing factor[1]. Unlike the ECO-AFA, which averages the link fuel consumption to compute real time-link cost factors ($FC'_{n,l} = (1 - \alpha)FC'_{n-1,l} + \alpha FC_{n,l}$), the proposed system adopts the eight variables instead and then allows each vehicle to compute its fuel consumption and build is optimum route in a decentralized fashion. It should be noted that the eight variables and eco-routes are updated only when a vehicle departs from its origin or exits a link; otherwise, route selection is based on the original routing solutions.

The updated eight variables are then updated using the vehicle-specific parameters and then input to the built-in energy consumption models (VT-CPFM and VT-CPEM) to estimate vehicle type-specific link costs. The results from the energy module are then used in the shortest path algorithm to compute the vehicle's minimum path. It should be noted that in this study we assume that drivers follow the computed optimum routes. A future study could investigate variability in driver response to route suggestions.

The routing decisions alter the network-wide traffic conditions, which in turn may affect the eco-routing solutions for subsequent iterations, and so forth. Accordingly, the system is a closed-loop feedback system that is able to generate real-time routing suggestions that adapt to the network-wide state evolution.

6.3. System testing

The simulation-based eco-routing system was tested on a sample hypothetical and a real network. Four vehicle types were selected to represent a typical vehicle fleet: Honda Accord (gasoline sedan car), Ford Expedition (gasoline SUV), International/ 9800 SBA (diesel truck), and Tesla S (electric LDV). It should be noted that a transit bus was not tested in this section given that buses typically operate on fixed routes. The system measures of effectiveness (MOEs) evaluated included: the energy consumption, travel time and distance traveled. These MOEs were compared to INTEGRATION's traditional eco-routing system (ECO-AFA) and travel time (TT) routing logic (AFA) both of which are built-in dynamic agent-based traffic assignment methods, as previously described. The differences in MOEs between the routing systems as a function of congestion level were also investigated.

[1] A default value of 0.2 is currently used in INTEGRATION.

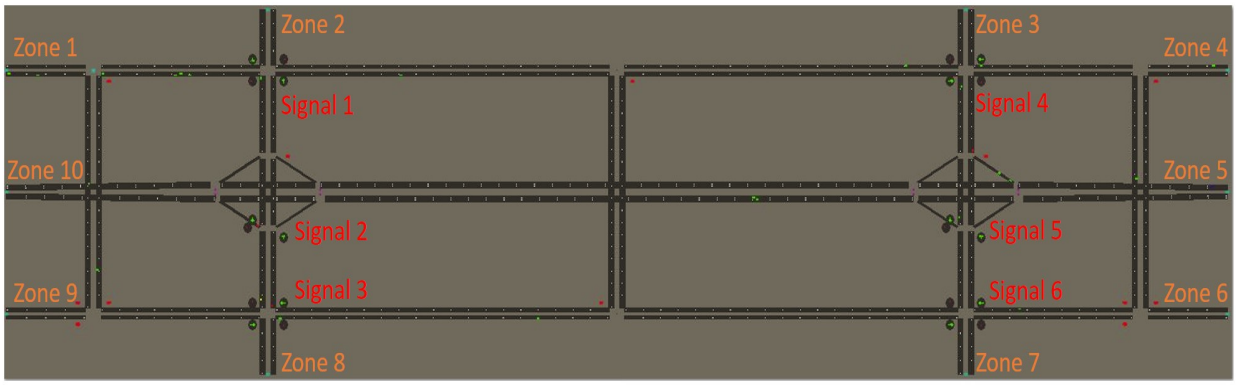

Fig. 4: QNET sample network

6.3.1. System testing on a sample network

The testing effort was first conducted on a sample network "QNET", consisting of 10 zones, 32 nodes, 68 links, and 49 OD pairs. The network includes traffic control infrastructure such as traffic signals and stop signs. As illustrated in Fig.4, the two central horizontal roads are freeways with a free-flow speed of 110 km/h and other roads are arterial roads with a free-flow speed of 60 km/h. The freeways have three lanes in each direction connected by one-lane on- and off-ramps, and each of the arterial roads has two lanes per direction.

An original demand of 2,500 veh/h was loaded onto the network for the first 1,800 s, and the simulation was continued until all of the loaded vehicles cleared the network. This resulted in a total of 1250 vehicles being simulated. Noticeably, the demand for each OD pair was equally shared by the four tested vehicle models in order to exclude the impact of disproportionate vehicle lineup on testing results. The simulation was run with 10 random seeds for each of the three routing methods. The MOEs relative to each routing method were calculated by dividing the total network statistics by the total number of vehicles, and then averaged over the 10 random seeds, as demonstrated in Table 6 that summarizes the average MOEs including travel distance (km), travel time (s), conventional fuel consumption (l), and electric energy consumption (Wh). The negative relative differences (Relative Diff.) in the table demonstrate lower MOEs for the proposed eco-routing, or vice versa.

According to the mean values in Table 6, the proposed eco-routing method on average produces conventional fuel usage of 0.453 l and an electric energy of 88.907 Wh. This results in energy savings of 4.5% for conventional fuel and 10.32% for electric power compared to the ECO-AFA system, and 4.22% (conventional fuel) and 22.09% (electric power) compared to the TT-AFA system. Furthermore, these results were statistically significant at a 5% significance level. In addition, the TT-AFA routing results in lower travel

time and shorter distances traveled yet more energy consumption, demonstrating that the minimum travel time or shortest distance route may produce higher energy consumption levels, confirming the findings in Ahn and Rakha (2008).

The method was also tested for multiple demand levels in order to quantify the impact of traffic congestion on the eco-routing system performance. Specifically, nine demand levels were tested by varying the traffic demand from 5% to 200% the original demand. At each demand level, the simulation was run 10 times using 10 random seeds for each of the three routing methods (a total of 30 simulation runs were completed for each demand level). The MOEs were then averaged over the random seeds. The average statistics were compared between the proposed eco-routing and the other two routing methods.

The results are presented in Table 7 in which the negative relative differences also demonstrate either energy, travel time or distance savings resulting from the proposed method. Basically, the proposed method produces the lowest energy consumption levels for both conventional and electric vehicles for all demand scenarios, demonstrating that the system in general outperforms traditional eco-routing and travel time routing methods.

Specifically, with an increasing demand level, the conventional fuel savings vary, on average, from 3.33% to 9.57% relative to the Eco-AFA system and from 6.92% to 0.76% relative to the TT-AFA system. The decreasing fuel savings relative to the TT-AFA routing are mainly attributed to the fact that fewer route alternatives are available for conventional vehicles when the network is congested. Compared to Eco-AFA routing, although more fuel savings are observed with increasing demands, it is still premature to claim that the proposed eco-routing algorithm achieves more fuel savings in a congested network. This is because the Eco-AFA routing's higher fuel consumption levels result from the fact that this system cannot tailor the eco-routes to the specific vehicle types and may generate incorrect link costs and eco-routes, routing vehicles along sub-optimal paths. Such routing error is considerably random and not monotonically related to the traffic congestion level.

For electric powered vehicles, the energy savings achieved by the proposed eco-routing algorithm do not demonstrate a monotonic increase or decrease with increased traffic demand. Specifically, the energy savings relative to the Eco-AFA system in general increase at first and then decrease with increasing congestion levels. The differences in energy consumption between the proposed eco-routing and the traditional Eco-AFA routing are as aforementioned considerably do not appear to be related to congestion levels. The savings relative to the TT-AFA method do not significantly vary with demand levels as well. This is, on the one hand, attributed to the fact that, in an uncongested network, electric vehicles would, in most cases, choose local roads to minimize their energy consumption levels given their significantly lower optimum energy economy cruise speeds (15-25 km/h, Wu et al. (2014a)), while they may choose the routes with higher traveling speeds such as freeways to minimize travel time. This may result in significant differences in

Table 6: Network-wide impacts of the proposed eco-routing method (sample network: QNET)

MOEs	Proposed Eco-routing (Pro-Eco)			ECO-AFA			TT-AFA			Relative Diff.	Relative Diff.
	Mean	Lower 95% CI	Upper 95% CI	Mean	Lower 95% CI	Upper 95% CI	Mean	Lower 95% CI	Upper 95% CI	(Pro-Eco vs. ECO-AFA: %)	(Pro-Eco vs. TT-AFA: %)
Distance (km)	3.298	3.292	3.304	3.488	3.454	3.523	3.177	3.166	3.187	-5.46	3.82
Travel time (s)	221.077	220.006	222.149	248.981	242.971	254.991	179.541	178.824	180.258	-11.21	23.13
fuel (l)	0.453	0.450	0.456	0.474	0.471	0.477	0.473	0.470	0.476	-4.50	-4.22
energy (Wh)	88.907	87.700	90.113	99.142	95.688	102.597	114.109	113.398	114.820	-10.32	-22.09

prevailing speeds and thus energy consumption between the two routing methods. On the other hand, in a congested network, electric vehicles regenerate more energy given frequent energy-producing deceleration events. Accordingly, electric vehicles may achieve significant energy savings at both low and high demand levels. This implies that electric vehicle eco-routing that only considers minimizing energy consumption may assign vehicles to congested networks, making traffic conditions even worse. Some constraints on other factors such as travel time are thus needed in future studies.

Despite the energy savings, the proposed eco-routing results in longer travel times (20.44%-29.81% more) and distances (2.38%-4.08% more) compared to travel time routing, as illustrated in Table 7. Consequently, improved energy efficiency may be at the cost of longer travel times or distances.

6.3.2. System testing on a real world network

The testing work was also completed on a real world network. Fig.5 shows the testing network located in downtown Doha city[3] in Qatar which was originally built in INTEGRATION to evaluate transportation operational strategies. The Doha network consists of 48 zones, 174 nodes, 302 links, and 13,536 OD pairs, including a large amount of traffic control infrastructures. The network can reflect real-world traffic conditions in large metropolitan areas. There are three road types in the network, including freeways with a free flow speed of 105 km/h and arterial roads with free flow speeds of 80 and 65 km/h respectively. The two central horizontal roads are freeways and other roads are arterial streets. The terrain of the testing area is relatively flat and thus road grade was assumed to be zero in this study.

For the base testing scenario, a calibrated single-hour traffic demand was loaded onto the network, while running the simulation until all vehicles cleared the network. Again, the demand for each OD pair was equally shared by the four tested vehicle models. The simulation was runs were repeated 10 times using different random seeds for each of the three routing methods, and the resulting MOEs were generated by averaging the statistics over the 10 runs.

Table 8 presents the simulation results. The proposed eco-routing method produces, on average, a conventional fuel consumption of 0.49 l and electric power usage of 67.822 Wh, resulting in energy savings of 2.04% for conventional fuel and 7.57% for electric energy respectively relative to the Eco-AFA system, and 6.12% (conventional fuel) and 12.53% (electric energy), respectively relative to the TT-AFA system. Furthermore, as was the case with the QNET sample network, the non-overlapped CIs demonstrate a significant

[3]The Doha network was used because it is a readily available network built in INTEGRATION prior to this study.

Table 7: Impacts of congestion level on eco-routing benefits (sample network: QNET)

MOEs	Routing Methods	Demand Levels								
		5%	25%	50%	75%	100%	125%	150%	175%	200%
Fuel (l)	Pro-Eco	0.472	0.443	0.449	0.452	0.453	0.458	0.464	0.472	0.48
	ECO-AFA	0.488	0.46	0.465	0.471	0.474	0.485	0.5	0.517	0.53
	TT-AFA	0.507	0.475	0.474	0.473	0.473	0.473	0.476	0.478	0.483
	Relative Diff. (Pro-Eco Vs. ECO-AFA) (%)	-3.33	-3.66	-3.56	-4.1	-4.5	-5.46	-7.05	-8.78	-9.57
	Relative Diff. (Pro-Eco Vs. TT-AFA) (%)	-6.92	-6.73	-5.26	-4.52	-4.22	-3.16	-2.51	-1.31	-0.76
Electric Energy (Wh)	Pro-Eco	91.653	93.698	92.972	91.503	88.907	88.38	86.06	83.395	80.837
	ECO-AFA	92.838	100.595	99.796	99.746	99.142	101.561	96.872	88.979	88.136
	TT-AFA	120.641	117.369	114.72	115.502	114.109	112.692	111.431	111.286	110.081
	Relative Diff. (Pro-Eco Vs. ECO-AFA) (%)	-1.28	-6.86	-6.84	-8.26	-10.32	-12.98	-11.16	-6.28	-8.28
	Relative Diff. (Pro-Eco Vs. TT-AFA) (%)	-23.05	-20.17	-18.96	-20.78	-22.09	-21.57	-22.77	-25.06	-26.57
Travel Time (s)	Pro-Eco	217.826	211.751	215.353	218.257	221.077	224.566	230.301	236.548	245.27
	ECO-AFA	214.014	224.872	228.762	240.489	248.981	260.205	286.571	319.344	352.9
	TT-AFA	174.792	175.808	177.186	177.629	179.541	180.385	182.988	185.112	188.952
	Relative Diff. (Pro-Eco Vs. ECO-AFA) (%)	1.78	-5.83	-5.86	-9.24	-11.21	-13.7	-19.64	-25.93	-30.5
	Relative Diff. (Pro-Eco Vs. TT-AFA) (%)	24.62	20.44	21.54	22.87	23.13	24.49	25.86	27.79	29.81
Distance (km)	Pro-Eco	3.407	3.302	3.306	3.308	3.298	3.286	3.277	3.258	3.245
	ECO-AFA	3.275	3.206	3.190	3.178	3.177	3.162	3.163	3.162	3.169
	TT-AFA	3.408	3.444	3.446	3.487	3.488	3.513	3.509	3.491	3.490
	Relative Diff. (Pro-Eco Vs. ECO-AFA) (%)	-0.02	-4.12	-4.07	-5.13	-5.46	-6.47	-6.61	-6.69	-7.04
	Relative Diff. (Pro-Eco Vs. TT-AFA) (%)	4.05	2.98	3.63	4.08	3.82	3.90	3.63	3.03	2.38

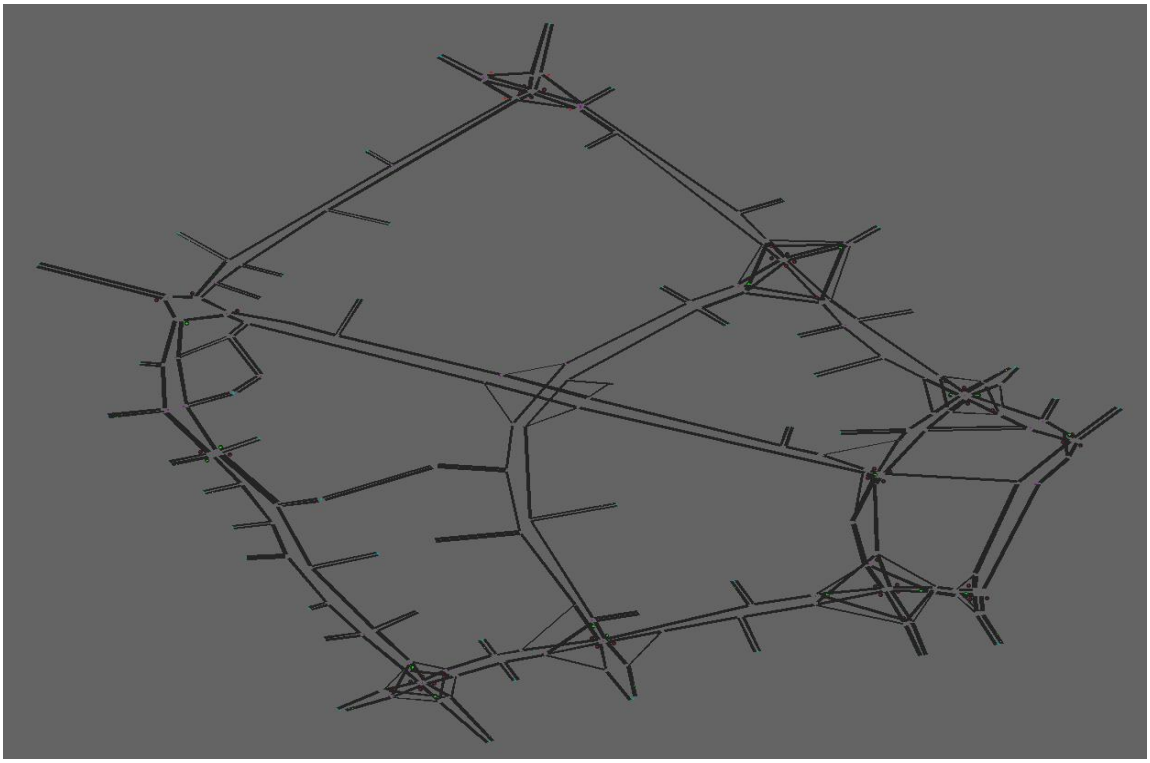

Fig. 5: Doha network

improvement by the proposed method in terms of energy efficiency. It is worth noting that, compared to the TT-AFA routing, the proposed eco-routing also results in shorter distance (-6.47%) and insignificant difference in travel time (-0.04%). This result is different from that generated in the QNET network in which longer distance and higher travel times were observed for the proposed eco-routing system. This demonstrates that, in some networks, the most energy-efficient routes may also achieve the optimum travel distance or time. Consequently, it can be concluded that network configuration significantly affects the eco-routing benefits and impacts.

Testing was also done for multiple demand levels. Again, nine demand levels were tested varying from 5% to 200% of the base scenario demand. At each demand level, the simulation was run 10 times with different random seeds for each of the routing methods. The MOEs were then averaged over the 10 runs and compared between the routing methods. The results are illustrated in Table 9.

The proposed eco-routing achieves energy savings for both conventional and electric vehicles at all demand levels. Specifically, the conventional fuel savings on average vary from 1.68% to 10.2% relative to the Eco-AFA system and from 0.83% to 7.69% relative to the TT-AFA system; and the electric energy savings vary from 1.02% to 9.09% relative to the Eco-AFA system and from 2.44% to 15.44% relative to the TT-AFA system. With increasing demand levels, the conventional fuel savings relative to the travel time routing decrease in general, although slight fluctuations are observed at some of the demand levels; while for electric vehicles, high energy savings are also achieved during congestion given that more deceleration events may occur in a congested network, resulting in increased energy regeneration. Noticeably, with increasing demands, the conventional fuel savings relative to the Eco-AFA system do not demonstrate a monotonic increase as was the case in the QNET sample network. This demonstrates that the energy savings of the proposed method relative to the traditional eco-routing logic vary with congestion levels.

It is worth noting that the electric energy savings relative to the TT-AFA system are significantly greater in the QNET network (shown in Table 7) than in the Doha network (shown in Table 9). This is probably attributable to the difference in network configurations. Specifically, there are three road types in the Doha network with a difference in free-flow speeds (65 km/h, 80 km/h, and 105 km/h) less significant than in the QNET network which had only two road types (60 km/h and 110 km/h). As demonstrated by a recent study Wu et al. (2014a), electric power is highly sensitive to cruise speed as illustrated in Figure 6. The vehicles cruising on freeways thus may produce significantly higher energy consumption levels compared to those cruising on arterial or local roads with lower prevailing speeds. In the QNET network, the majority of vehicles traveled on freeways for the travel time routing, while they chose arterial routes when routed in a fuel-efficient manner, resulting in a significant difference in energy consumption between the

Table 8: Network-wide impacts of the proposed eco-routing method (Doha network)

MOEs	Proposed Eco-routing (Pro-Eco)			ECO-AFA			TT-AFA			Relative Diff.	Relative Diff.
	Mean	Lower 95% CI	Upper 95% CI	Mean	Lower 95% CI	Upper 95% CI	Mean	Lower 95% CI	Upper 95% CI	(Pro-Eco vs. ECO-AFA: %)	(Pro-Eco vs. TT-AFA: %)
Distance	2.455	2.452	2.459	2.540	2.528	2.552	2.625	2.614	2.636	-3.33	-6.47
Travel time	227.639	226.611	228.667	236.280	233.623	238.937	227.723	224.589	230.857	-3.66	-0.04
fuel	0.490	0.486	0.494	0.500	0.497	0.503	0.522	0.516	0.527	-2.04	-6.12
energy	67.822	66.909	68.735	73.379	72.124	74.634	77.537	76.298	78.775	-7.57	-12.53

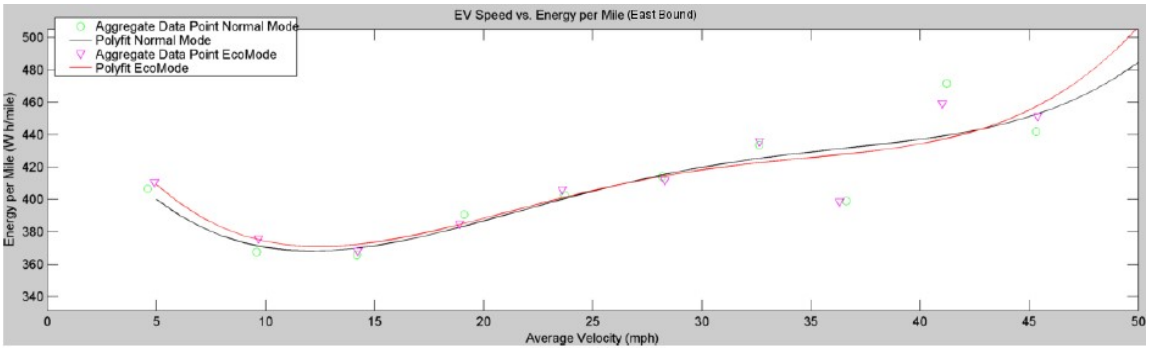

Fig. 6: Electric energy consumption vs. cruise speed

two routing methods. In the Doha network, however, the smaller significant difference in prevailing speeds resulted in lower energy savings.

For conventional fuel savings, there is no significant difference between the two tested networks. This is because conventional fuel consumption is less sensitive to the vehicle cruise speed compared to electric power. Specifically, as demonstrated in Fig.7 Wang and Rakha (2017a), fuel consumption produces a milder variation with cruise speed at most of the speed levels compared to electric power as illustrated in Fig.6. Network configuration also significantly affects conventional fuel savings resulting from eco-routing. For example, a grid network, given more route alternatives, may generate more fuel benefits compared to a freeway corridor network Ahn and Rakha (2013). Also, steep roads may be less attractive for eco-routing than flat roads. In addition, as demonstrated in Table 9, the proposed eco-routing method also results in shorter distances and lower travel times in the Doha network, which is different from the QNET results illustrated in Table 7. Accordingly, in some networks, the most energy-efficient routes may also achieve the optimum in travel times and distances; while in other networks, energy savings may be at the cost of longer distances or higher travel times.

7. Discussion

The application of the proposed eco-routing model hinges on the availability of the eight vehicle-agnostic link-specific variables computed based on the experiences of a sample or all vehicles. In this study, the INTEGRATION software tracked vehicle activities to compute and communicate (via wireless communication) these eight variables to the cloud for fusion with information gathered from other vehicles on the network. This information was then fed back to the vehicles via wireless communication. The vehicles then computed their unique optimum routes (edge computing). This architecture allows for a decentralized distributed traffic assignment system that requires minimum computational

Table 9: Impacts of congestion level on eco-routing benefits (Doha network)

MOEs	Routing Methods	Demand Levels								
		5%	25%	50%	75%	100%	125%	150%	175%	200%
Fuel (l)	Pro-Eco	0.252	0.410	0.454	0.474	0.490	0.508	0.527	0.558	0.598
	ECO-AFA	0.268	0.420	0.463	0.482	0.500	0.520	0.542	0.622	0.621
	TT-AFA	0.266	0.445	0.488	0.502	0.522	0.539	0.558	0.580	0.603
	Relative Diff. (Pro-Eco vs. ECO-AFA) (%)	-5.84	-2.23	-1.92	-1.68	-2.04	-2.30	-2.64	-10.20	-3.74
	Relative Diff. (Pro-Eco vs. TT-AFA) (%)	-5.28	-7.69	-7.02	-5.60	-6.12	-5.69	-5.43	-3.77	-0.83
Electric Energy (Wh)	Pro-Eco	38.790	66.961	70.580	70.097	67.822	65.494	63.203	61.258	58.294
	ECO-AFA	39.190	72.123	76.965	76.374	73.379	71.912	69.135	65.812	64.120
	TT-AFA	40.172	74.925	79.286	79.641	77.537	74.250	72.734	70.951	68.941
	Relative Diff. (Pro-Eco vs. ECO-AFA) (%)	-1.02	-7.16	-8.30	-8.22	-7.57	-8.92	-8.58	-6.92	-9.09
	Relative Diff. (Pro-Eco vs. TT-AFA) (%)	-2.44	-10.63	-10.98	-11.98	-12.53	-11.79	-13.10	-13.66	-15.44
Travel Time (s)	Pro-Eco	126.580	189.919	206.711	218.189	227.639	240.925	259.587	303.469	392.192
	ECO-AFA	130.099	192.410	211.831	224.627	236.280	253.878	281.916	414.346	466.813
	TT-AFA	133.052	198.566	213.447	219.518	227.723	240.938	263.723	317.186	396.323
	Relative Diff. (Pro-Eco vs. ECO-AFA) (%)	-2.70	-1.29	-2.42	-2.87	-3.66	-5.10	-7.92	-26.76	-15.99
	Relative Diff. (Pro-Eco vs. TT-AFA) (%)	-4.86	-4.35	-3.16	-0.61	-0.04	-0.01	-1.57	-4.32	-1.04
Distance (km)	Pro-Eco	1.211	2.116	2.343	2.405	2.455	2.486	2.511	2.543	2.582
	ECO-AFA	1.240	2.162	2.412	2.482	2.540	2.585	2.612	2.638	2.675
	TT-AFA	1.252	2.284	2.511	2.566	2.625	2.645	2.673	2.711	2.747
	Relative Diff. (Pro-Eco vs. ECO-AFA) (%)	-2.32	-2.16	-2.85	-3.07	-3.33	-3.84	-3.86	-3.60	-3.48
	Relative Diff. (Pro-Eco vs. TT-AFA) (%)	-3.24	-7.38	-6.68	-6.25	-6.47	-6.02	-6.06	-6.17	-6.01

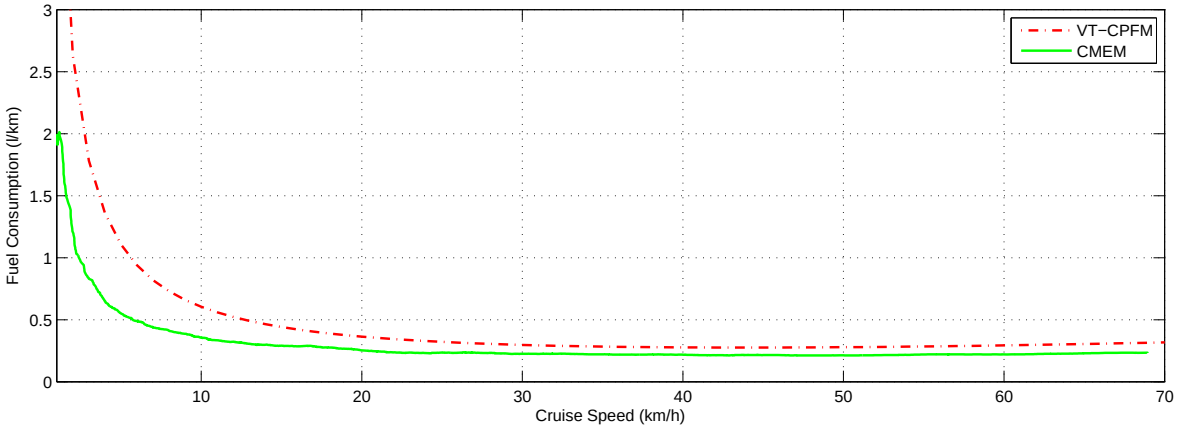

Fig. 7: Conventional fuel consumption vs. cruise speed

power on the cloud and all routing computations done in the vehicles (edge computing). In the simulation environment, however, all computations were made on a single server, given that all vehicles were tracked in the system resulting in the use of significant computational resources. Further enhancements to the model could be achieved through running on multiple processors.

The feasibility of the proposed eco-routing method with limited availability of feedback information was also investigated. Specifically, we explored a mesoscopic link cost function that attempted to mathematically relate each of the eight variables to the link congestion levels (quantified using the traffic stream density), so that link costs can be determined without feeding back the information once density is communicated. To this end, INTEGRATION was run on the QNET network to output the eight variables and density at five-minute intervals. These five-minute average statistics were then categorized by road type (freeway and arterial roads). Results demonstrated that, five of the eight parameters ($\sum_t VSP_{rga}^{(+)}(t)$, $\sum_t VSP_{rga}^{2(+)}(t)$, $\sum_t (VSP_{rga}^{(+)}(t) \cdot v^3(t)^{(+)})$, $\sum_t (VSP_{rga}^{(-)}(t) \cdot \eta_{re}(t))$, $\sum_t (v^3(t)^{(-)} \cdot \eta_{re}(t))$) exhibited no relationship with the roadway traffic stream density. Fig. 8 provides an example result that characterizes the relationship between each of the eight parameters and the link traffic density on freeways with a 90 km/h speed limit (average speed vs. density is also included). Specifically, the travel time per unit distance varies as a second-order polynomial function of density, and $\sum_t v^3(t)^{(+)}$ and $\sum_t v^6(t)^{(+)}$ exhibit a similar relationship. However, the other five parameters do not appear to exhibit an explicit mathematical relationship with density. This is mainly attributed to the fact that these parameters are significantly affected by vehicle acceleration levels, which is unrelated to link aggregated statistics (e.g. *density and average speed*). Consequently,

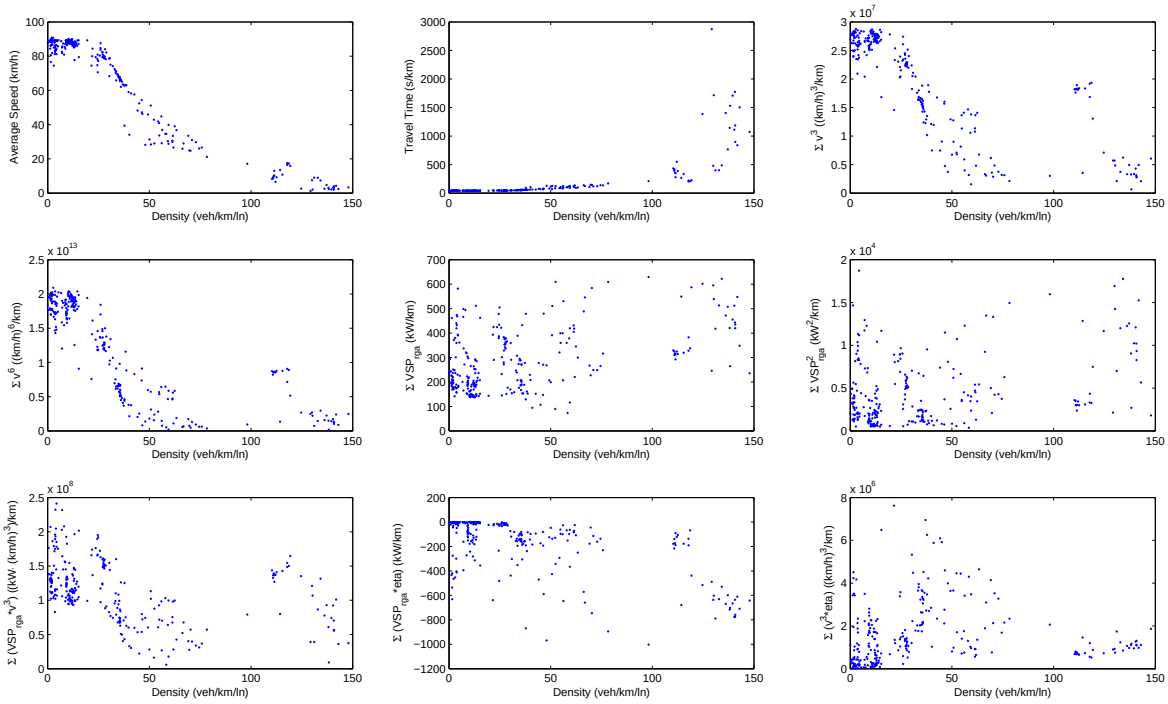

Fig. 8: Eight parameters vs. congestion level

the proposed eco-routing method may not be feasible when wireless communication is not available. With the advancement and popularization of vehicle connectivity, we envision this not being an issue.

8. Conclusions

The paper develops a novel dynamic eco-routing model designed for on-board navigation systems for conventional fuel- and electric-powered vehicles. Unlike previous efforts, the proposed model captures vehicle transient behavior along a link and allows for vehicle-specific routing decisions. The proposed model is formulated as a constrained non-linear optimization problem. The model was incorporated and tested in the INTEGRATION micro-simulation framework.

The results of the numerical experiment demonstrate that the model estimates are more robust compared to those of traditional models, which inadequately retain transient behavior and are unable to provide route recommendations tailored to specific vehicle types. The

results demonstrate that eco-routing using historical information produces sub-optimal route guidance.

Results of the simulation testing demonstrate that the proposed dynamic eco-routing method produces lower network-wide energy consumption levels compared to traditional eco-routing and travel time routing methods for different congestion levels. Furthermore, conventional fuel savings relative to travel time routing are found to decrease with increasing congestion levels given fewer route alternatives available in congested conditions. Electric power savings, however, relative to travel time routing, do not vary monotonically with congestion level given that significant savings could be achieved at both low and high traffic traffic demand levels. Neither are energy savings relative to traditional eco-routing monotonically related to congestion level. The results also demonstrate that the transportation network configuration significantly affects eco-routing benefits. In some networks, energy savings may be achieved at the cost of more travel time or distances traveled; while in other networks, eco-routes are also the most efficient in terms of travel times and distances.

The application of the proposed eco-routing method requires real-time vehicle communication to and from the cloud. Given that most vehicles are currently designed to have WiFi and cellular network connectivity, this should not be a problem from an implementation standpoint.

9. Recommendations for further research

The following are recommendations for further research:

Firstly, the model could be extended to consider pollutant emission-optimized routing in order to include air quality implications in the context of route planning. It should be noted, however, that and energy optimum route would result in the CO_2 optimized route given that CO_2 is directly related to fuel consumption.

Secondly, this study assumed full traveler compliance to the recommended routes. Numerous route choice studies, however, have demonstrated that drivers may not always follow the suggested optimum routes Ben-Elia et al. (2008); Ben-Elia and Shiftan (2010); Wang and Rakha (2015). For example, some drivers may avoid routes traversing downtown areas or university campuses even though they are informed that these routes are the best; some may prefer to choose habitual routes or rural routes. Future work could consider different driver compliance rates.

Thirdly, the proposed model considers a single objective, namely energy consumption. Future work could consider a multi-objective router given that travelers may not be willing to increase their travel time significantly to reduce their energy consumption. Consequently, constraining the eco-routing problem within reasonable travel times or distances would be another worthwhile future endeavor.

Fourthly, like many ITS systems, the proposed system utilizes vehicle communication capability (V2X) to communicate the vehicle-agnostic link-specific variables to the traffic management center. In this paper, we assume an ideal communication network. The authors in Elbery et al. (2015); Elbery and Rakha (2018), Elbery and Rakha (2019) have built a communication model in the INTEGRATION software that would allow for the testing of the eco-routing system in a realistic communication environment where packets may be dropped or delayed. Thus, another extension to this work is to evaluate the system performance within the context of realistic communication network constraints.

Finally, only four vehicle types were tested in the simulation. Future work could consider increasing the number of classes.

Acknowledgements

This effort was funded by the Office of Energy Efficiency and Renewable Energy (EERE), Vehicle Technologies Office, Energy Efficient Mobility Systems Program under award number DE-EE0008209 (DOE-VT-0008209-J02).

References

Ahn, K., Rakha, H., 2008. The effects of route choice decisions on vehicle energy consumption and emissions. Transportation Research Part D: Transport and Environment 13 (3), 151–167.

Ahn, K., Rakha, H., Trani, A., Van Aerde, M., 2002. Estimating vehicle fuel consumption and emissions based on instantaneous speed and acceleration levels. Journal of transportation engineering 128 (2), 182–190.

Ahn, K., Rakha, H. A., 2013. Network-wide impacts of eco-routing strategies: a large-scale case study. Transportation Research Part D: Transport and Environment 25, 119–130.

Barth, M., Boriboonsomsin, K., Vu, A., 2007. Environmentally-friendly navigation. In: Intelligent Transportation Systems Conference, 2007. ITSC 2007. IEEE. IEEE, pp. 684–689.

Ben-Elia, E., Erev, I., Shiftan, Y., 2008. The combined effect of information and experience on drivers route-choice behavior. Transportation 35 (2), 165–177.

Ben-Elia, E., Shiftan, Y., 2010. Which road do i take? a learning-based model of route-choice behavior with real-time information. Transportation Research Part A: Policy and Practice 44 (4), 249–264.

Benedek, C. M., Rilett, L. R., 1998. Equitable traffic assignment with environmental cost functions. Journal of Transportation Engineering 124 (1), 16–22.

Boriboonsomsin, K., Barth, M. J., Zhu, W., Vu, A., 2012. Eco-routing navigation system based on multisource historical and real-time traffic information. IEEE Transactions on Intelligent Transportation Systems 13 (4), 1694–1704.

Chen, A., Zhou, Z., Ryu, S., 2011. Modeling physical and environmental side constraints in traffic equilibrium problem. International Journal of Sustainable Transportation 5 (3), 172–197.

Chen, L., Yang, H., 2012. Managing congestion and emissions in road networks with tolls and rebates. Transportation Research Part B: Methodological 46 (8), 933–948.

De Nunzio, G., Sciarretta, A., Gharbia, I. B., Ojeda, L. L., 2018. A constrained eco-routing strategy for hybrid electric vehicles based on semi-analytical energy management. In: 2018 21st International Conference on Intelligent Transportation Systems (ITSC). IEEE, pp. 355–361.

De Nunzio, G., Thibault, L., Sciarretta, A., 2017. Model-based eco-routing strategy for electric vehicles in large urban networks. In: Comprehensive Energy Management–Eco Routing & Velocity Profiles. Springer, pp. 81–99.

Dijkstra, E. W., 1959. A note on two problems in connexion with graphs. Numerische mathematik 1 (1), 269–271.

Edwardes, W., Rakha, H., 2014. Virginia tech comprehensive power-based fuel consumption model: Modeling diesel and hybrid buses. Transportation Research Record: Journal of the Transportation Research Board (2428), 1–9.

Elbery, A., Rakha, H., 2019. City-wide eco-routing navigation considering vehicular communication impacts. Sensors 19 (2).
URL http://www.mdpi.com/1424-8220/19/2/290

Elbery, A., Rakha, H., Elnainay, M., Drira, W., Filali, F., Sep. 2015. Eco-routing using v2i communication: System evaluation. In: 2015 IEEE 18th International Conference on Intelligent Transportation Systems. pp. 71–76.

Elbery, A., Rakha, H., ElNainay, M. Y., Drira, W., Filali, F., 2016. Eco-routing: An ant colony based approach. In: Proceedings of the International Conference on Vehicle Technology and Intelligent Transport Systems - Volume 1: VEHITS,. INSTICC, SciTePress, pp. 31–38.

Elbery, A., Rakha, H. A., 2017. A novel stochastic linear programming feedback eco-routing traffic assignment system. Tech. rep.

Elbery, A., Rakha, H. A., May 2018. Vanet communication impact on a dynamic eco-routing system performance: Preliminary results. In: 2018 IEEE International Conference on Communications Workshops (ICC Workshops). pp. 1–6.

Ericsson, E., Larsson, H., Brundell-Freij, K., 2006. Optimizing route choice for lowest fuel consumption–potential effects of a new driver support tool. Transportation Research Part C: Emerging Technologies 14 (6), 369–383.

Fiori, C., Ahn, K., Rakha, H. A., 2016. Power-based electric vehicle energy consumption model: Model development and validation. Applied Energy 168, 257–268.

Fiori, C., Arcidiacono, V., Fontaras, G., Makridis, M., Mattas, K., Marzano, V., Thiel, C., Ciuffo, B., 2019. The effect of electrified mobility on the relationship between traffic conditions and energy consumption. Transportation Research Part D: Transport and Environment 67, 275–290.

Fitch, J. W., 1993. Motor truck engineering handbook. Training 2013, 08–05.

Houshmand, A., Cassandras, C. G., 2018. Eco-routing of plug-in hybrid electric vehicles in transportation networks. In: 2018 21st International Conference on Intelligent Transportation Systems (ITSC). IEEE, pp. 1508–1513.

Li, Q., Nie, Y., Vallamsundar, S., Lin, J. J., Homem-de Mello, T., 2013. Incorporating environmental measures into a reliable freight routing model. In: Transportation Research Board 92nd Annual Meeting. No. 13-4185.

Li, W., Wu, G., Yao, D., Zhang, Y., Barth, M. J., 2018. Dynamic en-route eco-navigation: Strategy design, implementation and evaluation. In: 2018 21st International Conference on Intelligent Transportation Systems (ITSC). IEEE, pp. 1888–1893.

Liu, C., Wu, J., Long, C., 2014. Joint charging and routing optimization for electric vehicle navigation systems. IFAC Proceedings Volumes 47 (3), 2106–2111.

Masikos, M., Demestichas, K., Adamopoulou, E., Theologou, M., 2014. Machine-learning methodology for energy efficient routing. IET Intelligent Transport Systems 8 (3), 255–265.

Masikos, M., Demestichas, K., Adamopoulou, E., Theologou, M., 2015. Energy-efficient routing based on vehicular consumption predictions of a mesoscopic learning model. Applied Soft Computing 28, 114–124.

Nagurney, A., 2000. Congested urban transportation networks and emission paradoxes. Transportation Research Part D: Transport and Environment 5 (2), 145–151.

Nagurney, A., Dong, J., 2002. A multiclass, multicriteria traffic network equilibrium model with elastic demand. Transportation Research Part B: Methodological 36 (5), 445–469.

Nie, Y. M., Li, Q., 2013. An eco-routing model considering microscopic vehicle operating conditions. Transportation Research Part B: Methodological 55, 154–170.

Park, S., Rakha, H., Ahn, K., Moran, K., 2013. Virginia tech comprehensive power-based fuel consumption model (VT-CPFM): model validation and calibration considerations. International Journal of Transportation Science and Technology 2 (4), 317–336.

Qi, X., Wu, G., Boriboonsomsin, K., Barth, M. J., 2018. Data-driven decomposition analysis and estimation of link-level electric vehicle energy consumption under real-world traffic conditions. Transportation Research Part D: Transport and Environment 64, 36–52.

Rakha, H., Ahn, K., Trani, A., 2004a. Development of VT-Micro model for estimating hot stabilized light duty vehicle and truck emissions. Transportation Research Part D: Transport and Environment 9 (1), 49–74.

Rakha, H., Lucic, I., Demarchi, S. H., Setti, J. R., Aerde, M. V., 2001. Vehicle dynamics model for predicting maximum truck acceleration levels. Journal of Transportation Engineering 127 (5), 418–425.

Rakha, H., Snare, M., Dion, F., 2004b. Vehicle dynamics model for estimating maximum light-duty vehicle acceleration levels. Transportation Research Record: Journal of the Transportation Research Board (1883), 40–49.

Rakha, H., Zhang, Y., 2004. INTEGRATION 2.30 framework for modeling lane-changing behavior in weaving sections. Transportation Research Record: Journal of the Transportation Research Board (1883), 140–149.

Rakha, H., Zhang, Y., 2006. Analytical procedures for estimating capacity of freeway weaving, merge, and diverge sections. Journal of transportation engineering 132 (8), 618–628.

Rakha, H. A., 2002. Integration release 2.30 for windows: Users guide–volume 1: Fundamental model features and volume 2: Advanced model features.

Rakha, H. A., Ahn, K., Moran, K., 2012. Integration framework for modeling eco-routing strategies: Logic and preliminary results. International Journal of Transportation Science and Technology 1 (3), 259–274.

Rakha, H. A., Ahn, K., Moran, K., Saerens, B., Van den Bulck, E., 2011. Virginia tech comprehensive power-based fuel consumption model: model development and testing. Transportation Research Part D: Transport and Environment 16 (7), 492–503.

Rilett, L., Van Aerde, M., MacKinnon, G., Krage, M., 1991. Simulating the TravTek route guidance logic using the INTEGRATION traffic model. In: Vehicle Navigation and Information Systems Conference. Vol. 2. IEEE, pp. 775–787.

Rilett, L. R., Benedek, C. M., 1994. Traffic assignment under environmental and equity objectives. Transportation Research Record: Journal of the Transportation Research Board (1443), 92–99.

Rilett, L. R., Van Aerde, M. W., 1991. Modelling distributed real-time route guidance strategies in a traffic network that exhibits the braess paradox. In: Vehicle Navigation and Information Systems Conference. Vol. 2. IEEE, pp. 577–587.

Saerens, B., Diehl, M., Van den Bulck, E., 2010. Optimal control using pontryagins maximum principle and dynamic programming. In: Automotive Model Predictive Control. Springer, pp. 119–138.

Shen, L., Shao, H., Wu, T., Lam, W. H., Zhu, E. C., 2019. An energy-efficient reliable path finding algorithm for stochastic road networks with electric vehicles. Transportation Research Part C: Emerging Technologies 102, 450–473.

Sugawara, S., Niemeier, D., 2002. How much can vehicle emissions be reduced?: exploratory analysis of an upper boundary using an emissions-optimized trip assignment. Transportation Research Record: Journal of the Transportation Research Board (1815), 29–37.

Tzeng, G. H., Chen, C.-H., 1993. Multiobjective decision making for traffic assignment. IEEE Transactions on Engineering Management 40 (2), 180–187.

Van Aerde, M., 1995. Single regime speed-flow-density relationship for congested and uncongested highways. In: 74th Annual Meeting of the Transportation Research Board, Washington, DC. Vol. 6.

Van Aerde, M., Rakha, H., 1995. Multivariate calibration of single regime speed-flow-density relationships [road traffic management]. In: Proceedings of Vehicle Navigation and Information Systems Conference. IEEE, pp. 334–341.

Van Aerde, M., Rakha, H., 2007. Integration© release 2.30 for windows: User's guide–volume I: Fundamental model features. M. Van Aerde & Assoc., Ltd., Blacksburg.

Van Aerde, M., Yagar, S., 1988. Dynamic integrated freeway/traffic signal networks: A routing-based modelling approach. Transportation Research Part A: Policy and Practice 22 (6), 445–453.

Wang, J., Rakha, H. A., 2015. Impact of dynamic route information on day-to-day driver route choice behavior. In: Transportation Research Board 94th Annual Meeting, No. 15-4918, Washington D.C.

Wang, J., Rakha, H. A., 2016a. Fuel consumption model for conventional diesel buses. Applied Energy 170, 394–402.

Wang, J., Rakha, H. A., 2016b. Heavy-duty diesel truck fuel consumption modeling. In: Transportation Research Board 95th Annual Meeting, No. 16-2147, Washington D.C.

Wang, J., Rakha, H. A., 2016c. Modeling fuel consumption of hybrid electric buses: Model development and comparison with conventional buses. Transportation Research Record: Journal of the Transportation Research Board (2539), 94–102.

Wang, J., Rakha, H. A., 2017a. Convex fuel consumption model for diesel and hybrid buses. Transportation Research Record: Journal of the Transportation Research Board, No. 2647.

Wang, J., Rakha, H. A., 2017b. Electric train energy consumption modeling. Applied Energy 193, 346–355.

Wang, J., Rakha, H. A., 2017c. Fuel consumption model for heavy duty diesel trucks: Model development and testing. Transportation Research Part D: Transport and Environment 55, 127–141.

Wang, J., Rakha, H. A., Fadhloun, K., 2017. Validation of the rakha-pasumarthy-adjerid car following model for vehicle fuel consumption and emission estimation applications. Transportation Research Part D: Transport and Environment 55, 127–141.

Wu, G., Boriboonsomsin, K., Barth, M. J., 2014a. Eco-routing navigation system for electric vehicles. Tech. rep., Center for Environmental Research and Technology, University of California, Riverside.

Wu, G., Boriboonsomsin, K., Barth, M. J., 2014b. Eco-routing navigation system for electric vehicles. Tech. rep., University of California, Riverside.

Yi, Z., Bauer, P. H., 2018. Optimal stochastic eco-routing solutions for electric vehicles. IEEE Transactions on Intelligent Transportation Systems (99), 1–11.

Yi, Z., Smart, J., Shirk, M., 2018. Energy impact evaluation for eco-routing and charging of autonomous electric vehicle fleet: Ambient temperature consideration. Transportation Research Part C: Emerging Technologies 89, 344–363.